Geochemistry Geophysics Geosystems G3
AN ELECTRONIC JOURNAL OF THE EARTH SCIENCES
Published by AGU and the Geochemical Society

Article
Volume 10, Number 8
5 August 2009
Q08002, doi:10.1029/2009GC002418
ISSN: 1525-2027

Ancient carbonate sedimentary signature in the Hawaiian plume: Evidence from Mahukona volcano, Hawaii

Shichun Huang
National High Magnetic Field Laboratory and Department of Geological Sciences, Florida State University, Tallahassee, Florida 32310, USA

Now at Department of Earth and Planetary Sciences, Harvard University, 20 Oxford Street, Cambridge, Massachusetts 02138, USA (huang17@fas.harvard.edu)

Wafa Abouchami
Max-Planck-Institut für Chemie, D-55128 Mainz, Germany

Janne Blichert-Toft
Laboratoire de Sciences de la Terre, UMR 5570, Ecole Normale Supérieure de Lyon, Université Claude Bernard Lyon 1, CNRS, 46 Allée d'Italie, F-69364 Lyon CEDEX 07, France

David A. Clague
Monterey Bay Aquarium Research Institute, Moss Landing, California 95039, USA

Brian L. Cousens
Ottawa-Carleton Geoscience Centre, Department of Earth Sciences, Carleton University, Ottawa, Ontario K1S 5B6, Canada

Frederick A. Frey
Department of Earth, Atmospheric and Planetary Sciences, Massachusetts Institute of Technology, 77 Massachusetts Avenue, Cambridge, Massachusetts 02139, USA

Munir Humayun
National High Magnetic Field Laboratory and Department of Geological Sciences, Florida State University, Tallahassee, Florida 32310, USA

[1] Lavas from Mahukona, a small Hawaiian volcano on the Loa trend, exhibit major and trace element abundance variations exceeding those in lavas from large Hawaiian shields, such as Mauna Loa and Mauna Kea. Mahukona lavas define three geochemically distinct groups of tholeiitic shield basalt and a transitional group of postsshield basalt. At 10% MgO the tholeiitic groups range from 9 to 12% CaO; such differences in CaO can reflect partial melts derived from garnet pyroxenite (low CaO) and peridotite (high CaO), but the negative CaO-Yb (both at 10% MgO) trend formed by Mahukona lavas is inconsistent with this explanation. Within Mahukona lavas, radiogenic Nd-Hf-Pb isotopic ratios are highly correlated with each other; however, $^{87}Sr/^{86}Sr$ is decoupled from these radiogenic isotopic ratios. Rather, $^{87}Sr/^{86}Sr$ is correlated with trace element abundance ratios involving Sr, and importantly, Mahukona lavas define a negative Rb/Sr-$^{87}Sr/^{86}Sr$ trend, implying that a Sr-rich source component characterized by high $^{87}Sr/^{86}Sr$ is important in the petrogenesis of Mahukona lavas. We infer that this Sr-rich source component is recycled ancient carbonate-rich sediments. Intershield heterogeneity among Hawaiian shields also shows a negative

Rb/Sr-$^{87}Sr/^{86}Sr$ trend. For example, Makapuu-stage Koolau lavas have higher $^{87}Sr/^{86}Sr$ but lower Rb/Sr than Mauna Kea lavas. Consequently, we infer that a recycled ancient carbonate-rich sedimentary source component is important in the Hawaiian plume. Although most lavas from Loa and Kea trend volcanoes define distinct fields in isotopic ratios of Sr, Nd, Hf, and Pb, the majority of Mahukona lavas have isotopic ratios at the boundary between the fields defined by Loa and Kea trend lavas. However, a subgroup of Mahukona shield lavas have Kea-like isotopic and trace element signatures, an observation that can be explained by vertical heterogeneity in a bilaterally asymmetrical plume.

Components: 16,428 words, 16 figures, 6 tables.

Keywords: mantle plume; Hawaii; carbonate; geochemical structure; radiogenic isotopes; chemical compositions.

Index Terms: 1025 Geochemistry: Composition of the mantle; 1038 Geochemistry: Mantle processes (3621); 1040 Geochemistry: Radiogenic isotope geochemistry.

Received 2 February 2009; **Revised** 10 June 2009; **Accepted** 15 June 2009; **Published** 5 August 2009.

Huang, S., W. Abouchami, J. Blichert-Toft, D. A. Clague, B. L. Cousens, F. A. Frey, and M. Humayun (2009), Ancient carbonate sedimentary signature in the Hawaiian plume: Evidence from Mahukona volcano, Hawaii, *Geochem. Geophys. Geosyst.*, *10*, Q08002, doi:10.1029/2009GC002418.

1. Introduction

[2] The Sr, Nd, Hf, Pb, Os and O isotopic variations in oceanic basalt reflect mantle heterogeneity that can be generated via mantle metasomatism [*Frey and Green*, 1974], recycling of oceanic [*Hofmann and White*, 1982] and continental crust [*Jackson et al.*, 2007] into the mantle, or delamination of lower continental crust [*McKenzie and O'Nions*, 1983]. Lavas forming the 0 to 80 Ma volcanoes along the age progressive Hawaiian-Emperor hot spot track show both temporal and spatial isotopic heterogeneity [e.g., *Roden et al.*, 1994; *Lassiter and Hauri*, 1998; *Keller et al.*, 2000; *Regelous et al.*, 2003]. Detailed studies indicate that the isotopic heterogeneity of Hawaiian-Emperor lavas is not a result of assimilation of oceanic lithosphere [e.g., *Eiler et al.*, 1996], but rather reflects geochemical heterogeneity within the Hawaiian plume [*Lassiter and Hauri*, 1998; *Blichert-Toft et al.*, 1999; 2003; *Abouchami et al.*, 2000; *Frey et al.*, 2005; *Huang et al.*, 2005a], with the exception that the assimilation of oceanic lithosphere into erupted Hawaiian lavas may be important in some West Maui and Kilauea lavas [*Gaffney et al.*, 2004; *Garcia et al.*, 2008]. The intrinsic isotopic heterogeneity of the Hawaiian plume has been interpreted in part as a manifestation of recycled, ancient oceanic lithosphere (including sediments) in the plume [e.g., *Hauri*, 1996; *Lassiter and Hauri*, 1998; *Blichert-Toft et al.*, 1999; *Jackson and Dasgupta*, 2008].

[3] From the island of Hawaii to Molokai and perhaps extending to Oahu, Hawaiian volcanoes form two subparallel spatial trends, the Loa and Kea trends (Figure 1). Lavas from these two volcanic trends show important differences in major and trace element abundances, and isotopic ratios. For example, *Abouchami et al.* [2005] showed that at a given $^{206}Pb/^{204}Pb$, Loa trend lavas have higher $^{208}Pb/^{204}Pb$, i.e., higher $^{208}Pb^*/^{206}Pb^*$, than Kea trend lavas. Loa and Kea trend lavas form different trends in plots of $^{208}Pb^*/^{206}Pb^*$ versus Sr, Nd and Hf isotopic ratios [*Abouchami et al.*, 2005; *Huang et al.*, 2005b]. Specifically, Kea trend lavas form horizontal trends in plots of $^{208}Pb^*/^{206}Pb^*$ versus Sr, Nd and Hf isotopic ratios. In contrast, Loa trend lavas form steep trends in these plots, with Makapuu-stage Koolau lavas (Oahu) defining the high $^{208}Pb^*/^{206}Pb^*$-$^{87}Sr/^{86}Sr$ and low $^{143}Nd/^{144}Nd$-$^{176}Hf/^{177}Hf$ end. Loa trend lavas, especially Makapuu-stage Koolau lavas, also have high La/Nb and Sr/Nb, which *Huang and Frey* [2005] and *Huang et al.* [2005b] proposed were derived from a recycled, ancient, carbonate-rich, phosphate-bearing sedimentary source component. In this paper, we present major and trace element abundances, and Sr-Nd-Hf-Pb isotopic data for lavas from Mahukona volcano, a submarine Loa trend Hawaiian volcano between Hualalai and

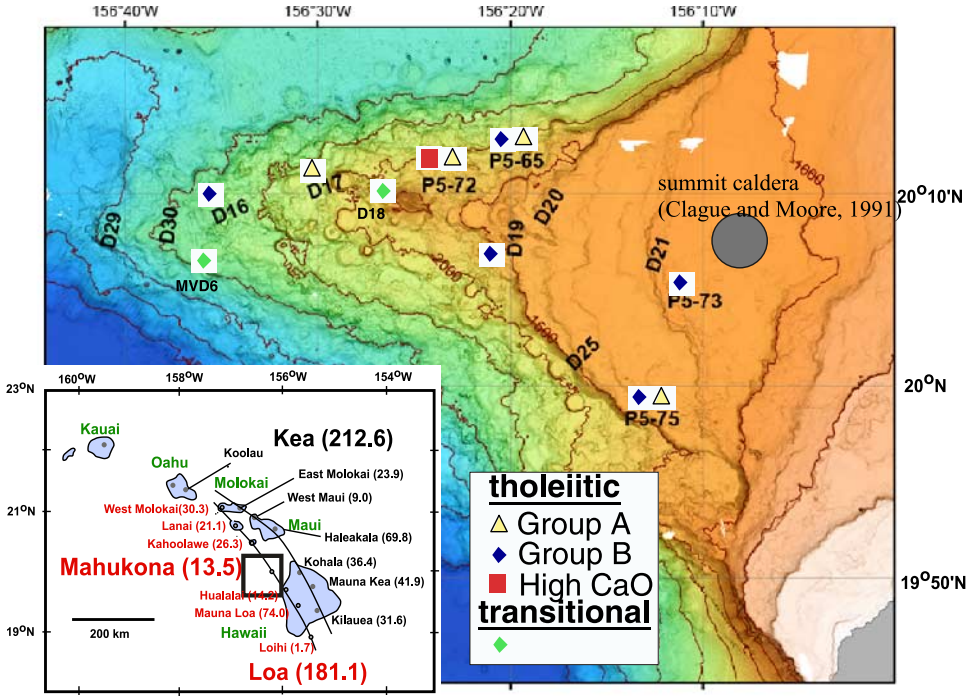

Figure 1. Map of Mahukona volcano. The inset shows Hawaiian islands (green) and Kea and Loa trend volcanoes (black and red, respectively). Volumes (in thousands of km^3) of each volcano estimated by *Robinson and Eakins* [2006] are given. The locations of the analyzed Mahukona lavas are shown on the colored map (black box in inset).

Kahoolawe (Figure 1). Using these data, we infer the source characteristics of Mahukona lavas, and discuss their implications for the geochemical structure of the Hawaiian plume.

2. Mahukona Volcano and Samples Studied

[4] Transitional and tholeiitic basaltic lavas have been recovered from Mahukona volcano [*Garcia et al.*, 1990; *Clague and Moore*, 1991a], with their classification based on a total alkalis versus SiO_2 plot [see *Clague and Calvert*, 2009, Figure 3]. The tholeiitic basalts represent the shield growth stage of Mahukona volcano, which ended between 410 and 500 ka [*Garcia et al.*, 1990; *Clague and Moore*, 1991a, 1991b; *Clague and Calvert*, 2009]. *Garcia et al.* [1990] classified the transitional basaltic lavas recovered from the large cone labeled D18 (Figure 1) as preshield stage lavas on the basis of their high $^3He/^4He$ (20–21 R/R_A) [*Garcia et al.*, 1990; *Garcia and Kurz*, 1991]. In contrast, *Clague and Moore* [1991a, 1991b] argued that the D18 transitional lavas are postshield lavas based mainly on a different interpretation for the location of the volcano summit. This inference has been confirmed by the relatively young ages of the transitional lavas from the D18 cone (298 ± 25 ka) and from dredge site D6 (310 ± 31 ka) on the west rift zone [*Clague and Calvert*, 2009] (Table 1 and Figure 1). This age range coincides with the transition from tholeiitic shield stage to alkalic postshield stage volcanism at Kohala, the Kea neighbor of Mahukona (Figure 1), which occurred between 300 and 260 ka [*McDougall and Swanson*, 1972; *Clague and Dalrymple*, 1987], and is much older than the postshield volcanism at Hualalai (the Loa neighbor of Mahukona; Figure 1), which started at 115 ka and is still active [*Moore and Clague*, 1992; *Cousens et al.*, 2003].

[5] Mahukona volcano has been sampled extensively during several cruises over the past 20 years [e.g., *Garcia et al.*, 1990; *Clague and Moore*, 1991a; *Clague and Calvert*, 2009]. However, most Mahukona samples have been analyzed only for major element compositions [*Garcia et al.*, 1990; *Clague and Moore*, 1991a]. In order to better characterize the geochemical compositions of Mahukona lavas, we selected 23 whole rock samples for major and trace element analyses, and 21 of these for Sr-Nd-Hf-Pb isotopic measurements (Tables 1–3, 4a, and 4b). The details of analytical procedures are in Appendix A. The locations (Figure 1) and sampling methods of most of the

Table 1. Major Element Contents in Mahukona Lavas[a]

Sample	Group	SiO_2	TiO_2	Al_2O_3	FeO	MnO	CaO	MgO	K_2O	Na_2O	P_2O_5	Total	LOI[b]	Age[c] (ka)
Transitional lavas														
F288HW-D18-6		46.71	2.38	13.26	12.58	0.18	10.55	10.80	0.42	2.28	0.24	99.40	−0.26	298 ± 25
D6-R3		47.00	2.59	13.99	12.33	0.18	11.12	9.55	0.51	2.48	0.26	100.00		310 ± 31
D6-R5		46.32	2.35	12.92	12.57	0.18	10.17	12.47	0.55	2.25	0.23	100.00		
D6-R6		46.36	2.36	12.77	12.48	0.18	10.11	12.77	0.48	2.25	0.24	100.00		
D6-R8		46.30	2.34	12.86	12.62	0.18	10.14	12.59	0.53	2.19	0.23	100.00		
Tholeiitic lavas														
F288HW-D17	A	51.34	2.49	12.68	10.71	0.17	9.16	9.42	0.49	2.50	0.31	99.27	−0.46	
P5-65-1	A	51.18	2.52	12.48	11.33	0.19	9.08	9.64	0.53	2.36	0.32	99.61	−0.14	
P5-65-5	A	51.49	2.39	12.58	10.23	0.18	9.07	10.64	0.46	2.35	0.30	99.69		
P5-72-5	A	49.34	2.01	11.09	11.13	0.17	8.30	15.17	0.35	2.05	0.23	99.84		
P5-72-5 DUP	A	48.74	1.95	10.86	11.21	0.17	7.98	15.07	0.34	2.06	0.23	98.61		
P5-72-7	A	50.27	2.34	11.96	11.76	0.18	8.69	11.62	0.45	2.28	0.29	99.83	−0.39	
P5-72-8	A	50.62	2.40	12.38	11.51	0.17	8.88	10.81	0.46	2.28	0.30	99.81	−0.28	
P5-75-1	A	50.87	2.69	13.02	11.52	0.17	9.52	8.65	0.47	2.47	0.31	99.70	−0.10	
P5-75-1 DUP	A	50.32	2.66	12.50	11.46	0.18	9.04	9.06	0.49	2.43	0.32	98.46		
F288HW-D16-2	B	46.65	1.46	8.26	11.60	0.16	6.56	23.11	0.23	1.34	0.15	99.52	−0.48	
F288HW-D16-2 DUP	B	46.88	1.45	8.24	11.75	0.17	6.56	23.04	0.23	1.36	0.15	99.82		
F288HW-D19-9	B	44.07	1.31	7.84	12.46	0.18	6.50	25.86	0.09	1.14	0.15	99.59	−0.16	
P5-65-6	B	50.10	2.29	12.62	11.43	0.17	10.00	10.01	0.36	2.06	0.24	99.28	−0.33	
P5-65-7	B	49.92	2.21	12.01	11.49	0.17	9.44	12.29	0.34	1.97	0.23	100.07	−0.38	
P5-65-8B	B	49.65	2.18	12.03	11.73	0.17	9.54	12.16	0.33	1.97	0.22	99.97	−0.29	
P5-73-3	B	50.50	2.32	13.28	11.49	0.17	10.28	8.95	0.40	2.19	0.24	99.81	0.12	
P5-73-4	B	47.02	1.30	8.35	11.67	0.16	6.58	23.54	0.19	1.37	0.13	100.31	0.18	
P5-73-5	B	47.99	1.52	9.77	11.46	0.16	7.64	19.71	0.22	1.59	0.16	100.22	0.18	
P5-75-4	B	50.23	2.16	12.50	11.38	0.17	9.99	11.02	0.34	2.13	0.25	100.17	−0.01	
P5-72-1	High CaO	49.50	1.42	13.69	9.50	0.16	12.19	9.91	0.38	1.86	0.15	98.76		
P5-72-3	High CaO	49.81	1.48	13.98	10.21	0.16	12.48	9.35	0.37	1.91	0.16	99.91	−0.26	

[a] Unit is percent.
[b] LOI, loss on ignition.
[c] Pooled Ar-Ar plateau ages from *Clague and Calvert* [2009].

studied samples are given by *Clague and Moore* [1991a], while those of the D6 samples are given by *Clague and Calvert* [2009].

3. Results

3.1. Major Elements

[6] It is well known that Hawaiian tholeiitic shield lavas exhibit important intershield heterogeneity in major element compositions [e.g., *Frey et al.*, 1994; *Hauri*, 1996]. For example, at a given MgO content most Mauna Loa shield stage lavas have lower CaO content and higher SiO_2 content than Mauna Kea shield stage tholeiitic lavas (Figure 2); a small group of Mauna Kea glasses (CaO-K_2O-rich group) have even higher CaO content than other Mauna Kea shield stage tholeiitic lavas [*Stolper et al.*, 2004]. Although Mahukona volcano has a much smaller volume than Mauna Loa or Mauna Kea (Figure 1) [*Robinson and Eakins*, 2006], whole rocks and glasses recovered from Mahukona show significant compositional variation [*Clague and Moore*, 1991a]. For example, Mahukona lavas have CaO contents that span the entire range covered by Mauna Loa and Mauna Kea shield stage tholeiitic lavas (Figure 2a). Mahukona tholeiitic lavas can be subdivided into three distinctive groups in an MgO-CaO plot (Figure 2a). In detail, Group A tholeiitic lavas have slightly lower CaO content than Mauna Loa lavas, and Group B tholeiitic lavas lie within the region of overlap between Mauna Loa and Mauna Kea shield stage tholeiitic lavas. The Mahukona high-CaO tholeiitic group lavas have CaO contents similar to that of Mauna Kea CaO-K_2O-rich glasses. Mahukona transitional lavas have CaO contents higher than Mauna Loa lavas, but are within the Mauna Kea shield stage tholeiitic field. In an MgO-SiO_2 plot (Figure 2b), Mahukona transitional lavas have lower SiO_2 contents than any Hawaiian shield stage tholeiitic lavas.

[7] There is no clear correlation between sample group and sample location (Figure 1). For example, transitional lavas have been recovered from three different locations (D18, D6 and D30) about 20 km

Table 2. Trace Element Abundances by XRF in Mahukona Lavas[a]

Sample	Group	Ni	Cr	V	Ba	Sr	Zr	Y	Nb	Cu	Zn
Transitional lavas											
F288HW-D18-6		320	434	299	76	312	129	28	13	88	112
D6-R3		270	404	307	97	347	141	29	12	87	114
D6-R5		442	541	285	86	318	130	27	11	92	111
D6-R6		449	549	282	86	314	129	27	11	85	111
D6-R8		450	559	277	90	317	129	27	11	83	112
Tholeiitic lavas											
F288HW-D17	A	274	481	288	84	264	176	33	14	106	98
P5-65-1	A	290	430	287	107	264	189	35	15	86	106
P5-65-5	A	356	581	285	88	313	170	33	14	87	97
P5-72-5	A	609	891	257	73	222	128	26	10	88	97
P5-72-7	A	408	592	274	92	256	163	32	13	87	101
P5-72-8	A	360	543	287	106	272	168	31	14	90	102
P5-75-1	A	197	482	322	81	283	178	35	15	95	104
F288HW-D16-2	B	1178	1160	191	35	173	84	17	8	66	88
F288HW-D16-2 DUP	B	1168	1158	205	46	174	83	18	7	72	89
F288HW-D19-9	B	1210	1622	180	11	178	72	17	7	46	93
P5-65-6	B	269	562	297	69	284	132	27	13	109	95
P5-65-7	B	401	690	279	72	268	126	25	11	102	94
P5-65-8B	B	382	712	272	70	269	124	24	10	107	92
P5-73-3	B	193	413	292	88	306	138	26	11	113	93
P5-73-4	B	1102	1462	180	20	195	76	15	7	80	91
P5-73-5	B	884	1441	209	28	218	87	18	8	103	91
P5-75-4	B	321	552	284	69	277	124	25	10	96	94
P5-72-1	High CaO	218	673	237	107	286	83	16.4	8.6		87
P5-72-3	High CaO	184	537	244	90	289	82	18	9	112	74

[a] Unit is ppm.

apart [*Clague and Calvert*, 2009], and both Group A and B lavas were recovered on P5–65 and P5–75 *Pisces V* submersible dives (Figure 1).

3.2. Trace Elements

[8] There are also important intershield heterogeneities in trace element abundances and ratios [e.g., *Lassiter et al.*, 1996; *Huang and Frey*, 2003]. At a given MgO content, Nb and Yb abundances increase in the order of Makapuu-stage Koolau < Mauna Loa < Mauna Kea tholeiitic shield stage (Figure 3). Mahukona tholeiitic lavas also show three distinctive groups in plots of MgO versus Nb and Yb, with Group A having the highest Nb and Yb abundances and the high-CaO group the lowest Nb and Yb abundances (Figure 3). In detail, Mahukona Group A tholeiitic lavas have Nb abundances similar to, and Yb abundances higher than, those in Mauna Kea shield stage tholeiitic lavas; Mahukona high-CaO lavas have Nb and Yb abundances similar to those in Makapuu-stage Koolau lavas.

[9] The ratio of Sr/Nb is another important intershield discriminator [*Frey et al.*, 1994]; for example, Mauna Loa shield stage tholeiitic lavas have higher Sr/Nb than Mauna Kea shield stage tholeiitic lavas (Figure 3c). However, Mahukona lavas range widely in Sr/Nb with Group A overlapping with Mauna Kea shield stage lavas and Group B and high-CaO lavas overlapping with Mauna Loa shield stage lavas (Figure 3c).

3.3. Radiogenic Isotopes

[10] In an $^{87}Sr/^{86}Sr$-$^{143}Nd/^{144}Nd$ plot (Figure 4), Mahukona lavas form clusters overlapping the Mauna Loa and Mauna Kea fields; in detail, however, $^{87}Sr/^{86}Sr$ is not correlated with $^{143}Nd/^{144}Nd$ within Mahukona lavas. In contrast to $^{87}Sr/^{86}Sr$, ε_{Nd} is highly correlated with ε_{Hf} in Mahukona lavas with $R^2 = 0.96$ (inset of Figure 5). Like other Hawaiian shields, the Mahukona $\varepsilon_{Nd} - \varepsilon_{Hf}$ trend is less steep than the global OIB array [e.g., *Blichert-Toft et al.*, 1999]. Among the Mahukona groups, the high-CaO group lavas have the lowest $^{143}Nd/^{144}Nd$ and $^{176}Hf/^{177}Hf$.

[11] *Abouchami et al.* [2005] showed that the Loa and Kea trend lavas are distinguishable, with minor overlap, in a $^{206}Pb/^{204}Pb$-$^{208}Pb/^{204}Pb$ plot with Loa trend lavas having higher $^{208}Pb/^{204}Pb$ at a given $^{206}Pb/^{204}Pb$ than Kea trend lavas [*Eisele et al.*, 2003; *Abouchami et al.*, 2005] (Figure 6). Mahukona Group B tholeiitic lavas straddle the Loa-Kea dividing line; Group A lavas plot on the Kea side;

Table 3. Trace Element Abundances by ICP-MS in Mahukona Lavas[a]

Sample	Group	Rb	Sr	Y	Nb	Ba	La	Ce	Pr	Nd	Sm	Eu	Gd	Tb	Dy	Ho	Er	Tm	Yb	Lu	Hf	Ta	Pb	Th	U
Transitional lavas																									
F288HW-D18-6		6.3	312	27.5	11.9	89	11.0	25.5	3.53	17.2	5.10	1.85	5.54	0.93	5.56	1.10	2.64	0.36	2.10	0.31	3.46	0.82	1.60	0.77	0.25
D6-R3		6.3	355	30.1	13.2	88	11.9	27.6	4.08	19.3	5.51	1.86	5.98	0.93	5.35	1.01	2.58	0.37	2.20	0.33	3.74	0.81	0.97	0.70	0.23
D6-R5		6.9	324	27.0	12.0	80	10.7	25.0	3.70	17.3	5.01	1.70	5.46	0.84	4.86	0.91	2.39	0.32	1.96	0.30	3.36	0.73	0.86	0.63	0.19
D6-R6		6.0	321	27.4	12.1	79	10.8	25.3	3.73	17.6	5.00	1.71	5.40	0.85	4.91	0.93	2.45	0.33	2.01	0.30	3.42	0.74	0.90	0.65	0.18
D6-R8		6.5	326	27.3	12.1	78	10.7	25.0	3.68	17.3	4.93	1.69	5.40	0.84	4.88	0.92	2.41	0.34	2.02	0.30	3.37	0.74	0.87	0.65	0.19
Tholeiitic lavas																									
F288HW-D17	A	9.0	278	35.5	13.1	107	13.5	31.9	4.54	22.3	6.81	2.36	7.55	1.28	7.21	1.38	3.38	0.46	2.65	0.37	4.82	0.91	1.26	1.43	0.30
P5-65-1	A	8.7	279	36.7	14.1	106	14.2	34.0	4.69	23.2	7.04	2.39	7.63	1.23	7.45	1.42	3.51	0.47	2.70	0.40	5.17	0.95	1.25	1.06	0.34
P5-65-5	A	7.3	328	34.2	13.0	99	13.3	31.2	4.38	21.7	6.63	2.20	7.11	1.16	7.04	1.35	3.36	0.46	2.54	0.38	4.87	0.90	1.49	0.96	0.31
P5-72-5	A	5.8	236	27.0	9.6	83	9.7	23.2	3.26	16.2	5.00	1.78	5.77	0.94	5.43	1.05	2.61	0.34	2.01	0.29	3.60	0.66	1.20	0.67	0.22
P5-72-7	A	7.4	264	32.5	12.1	100	12.2	29.1	4.03	20.1	6.20	2.12	6.96	1.14	6.55	1.27	3.15	0.42	2.37	0.34	4.40	0.83	1.44	0.86	0.32
P5-72-8	A	7.9	286	33.3	12.6	113	12.7	30.0	4.18	20.9	6.41	2.23	7.08	1.17	6.75	1.31	3.20	0.44	2.46	0.35	4.55	0.84	1.35	0.88	0.28
P5-75-1	A	7.5	293	35.8	12.8	98	13.1	31.4	4.39	21.9	6.78	2.42	7.76	1.25	7.24	1.37	3.40	0.46	2.62	0.39	4.98	0.91	1.50	0.95	0.29
F288HW-D16-2	B	3.5	179	17.9	6.3	46	6.1	14.9	2.13	10.9	3.32	1.17	3.62	0.61	3.65	0.69	1.74	0.24	1.34	0.19	2.25	0.44	0.62	0.43	0.13
F288HW-D19-9	B	0.9	181	16.6	6.0	27	5.9	13.4	1.92	9.5	2.94	1.06	3.27	0.54	3.26	0.62	1.56	0.21	1.18	0.18	1.94	0.40	0.58	0.39	0.18
P5-65-6	B	5.6	296	27.7	10.3	79	10.2	24.2	3.43	17.3	5.24	1.88	5.82	0.94	5.70	1.08	2.65	0.37	2.05	0.30	3.75	0.69	0.96	0.68	0.24
P5-65-7	B	5.4	280	26.0	9.6	78	9.5	22.7	3.24	16.3	5.01	1.88	5.70	0.95	5.37	1.02	2.56	0.34	1.89	0.28	3.47	0.67	1.02	0.73	0.22
P5-65-8B	B	5.0	277	25.3	9.4	78	9.2	22.1	3.13	15.7	4.92	1.78	5.42	0.88	5.19	0.98	2.50	0.33	1.85	0.28	3.31	0.64	1.06	0.63	0.21
P5-73-3	B	6.1	317	27.7	10.2	91	10.5	25.1	3.54	17.6	5.43	1.93	6.07	0.98	5.76	1.11	2.76	0.36	2.09	0.31	3.74	0.70	1.18	0.70	0.26
P5-73-4	B	2.7	200	15.2	5.1	36	5.4	13.0	1.85	9.3	2.89	1.07	3.23	0.55	3.15	0.61	1.53	0.20	1.16	0.16	1.99	0.35	0.63	0.37	0.13
P5-73-5	B	3.1	230	18.1	6.1	44	6.4	15.6	2.22	10.9	3.49	1.26	3.83	0.62	3.68	0.69	1.76	0.24	1.37	0.19	2.31	0.43	0.91	0.41	0.26
P5-75-4	B	5.1	288	25.5	9.3	77	9.6	23.0	3.21	16.1	4.97	1.79	5.43	0.91	5.24	1.00	2.46	0.33	1.91	0.28	3.43	0.65	1.03	0.61	0.23
P5-72-3	High CaO	6.1	294	17.7	8.3	87	7.7	17.4	2.32	11.1	3.27	1.19	3.46	0.57	3.60	0.68	1.71	0.23	1.30	0.19	2.15	0.58	0.84	0.52	0.17

[a] Unit is ppm.

Table 4a. Sr-Nd-Hf Isotopic Ratios in Mahukona Lavas

Sample	Group	$^{87}Sr/^{86}Sr$	2 Sigma	$^{143}Nd/^{144}Nd$	2 Sigma	$^{176}Hf/^{177}Hf$	2 Sigma
Transitional lavas							
F288HW-D18-6		0.703657	0.000007	0.512933	0.000005	0.283087	0.000004
F288HW-D18-6[a]						0.283091	0.000009
D6-R3		0.703737	0.000007	0.512925	0.000004	0.283087	0.000005
D6-R3[b]		0.703692	0.000006	0.512927	0.000005		
D6-R3[a]						0.283089	0.000005
D6-R6		0.703675	0.000007	0.512929	0.000002	0.283086	0.000005
D6-R6[b]		0.703677	0.000005	0.512921	0.000003		
D6-R6[a]						0.283086	0.000003
Tholeiitic lavas							
F288HW-D17	A	0.703593	0.000007	0.512981	0.000006	0.283118	0.000004
P5-65-1	A	0.703557	0.000006	0.512983	0.000006	0.283118	0.000004
P5-65-5	A	0.703565	0.000005	0.512985	0.000003	0.283120	0.000004
P5-72-5	A	0.703555	0.000005	0.512992	0.000002	0.283126	0.000004
P5-72-7	A	0.703565	0.000006	0.512987	0.000003	0.283124	0.000003
P5-72-8	A	0.703557	0.000005	0.512996	0.000004	0.283124	0.000004
P5-75-1	A	0.703572	0.000006	0.512987	0.000006	0.283128	0.000004
F288HW-D16-2	B	0.703610	0.000005	0.512984	0.000003	0.283122	0.000005
F288HW-D19-9	B	0.703764	0.000010	0.512971	0.000005	0.283117	0.000005
P5-65-6	B	0.703585	0.000005	0.512996	0.000003	0.283120	0.000004
P5-65-7	B	0.703589	0.000007	0.512987	0.000006	0.283129	0.000005
P5-65-8B	B	0.703584	0.000006	0.512990	0.000003	0.283131	0.000004
P5-73-3	B	0.703735	0.000009	0.512945	0.000006	0.283093	0.000003
P5-73-4	B	0.703819	0.000008	0.512939	0.000003	0.283094	0.000004
P5-73-5	B	0.703740	0.000007	0.512923	0.000008	0.283086	0.000004
P5-75-4	B	0.703730	0.000005	0.512946	0.000005	0.283094	0.000004
P5-72-1	high CaO	0.703671	0.000007	0.512898	0.000003	0.283071	0.000005
P5-72-3	high CaO	0.703643	0.000008	0.512893	0.000005	0.283070	0.000004
P5-72-3[a]	high CaO					0.283069	0.000002

[a] Hf isotopic analyses done at Florida State University.
[b] Sr-Nd isotopic analyses done at Carleton University.

the postshield transitional lavas plot within the Loihi field; the high-CaO tholeiitic group lavas are within the Kahoolawe field, and also have the lowest $^{206}Pb/^{204}Pb$ and $^{208}Pb/^{204}Pb$ among Mahukona lavas.

[12] The Loa-Kea difference in a $^{206}Pb/^{204}Pb$-$^{208}Pb/^{204}Pb$ plot can be expressed as $^{208}Pb^*/^{206}Pb^*$ [*Abouchami et al.*, 2005], which reflects the time-integrated $^{232}Th/^{238}U$ since the formation of the Earth and is defined as $[(^{208}Pb/^{204}Pb)_{sample} - 29.475]/[(^{206}Pb/^{204}Pb)_{sample} - 9.307]$ [*Galer and O'Nions*, 1985]. Similar to other Loa trend lavas, Mahukona lavas form a negative trend in a $^{208}Pb^*/^{206}Pb^*$-$^{176}Hf/^{177}Hf$ plot with $R^2 = 0.92$ (Figure 7).

4. Discussion

4.1. Geochemical Variations Within Mahukona Lavas: Incompatible Trace Element Abundances

[13] At a given MgO content, the groups of Mahukona shield lavas differ in incompatible element abundances (Figure 3). This result cannot be explained by fractionation of a common parental magma. If Mahukona lavas are compared at a common MgO content, such as 10%, which remove the effects of olivine fractionation/accumulation [e.g., *Langmuir et al.*, 1992], they form linear trends in plots of $[Nb]_{10}$ versus $[La]_{10}$ and $[Yb]_{10}$ (element abundances at 10% MgO) (Figure 8). In detail, $[Nb]_{10}$ ranges from 8.07 to 14.0 ppm, a factor of 1.74; $[La]_{10}$ from 7.51 to 14.1 ppm, a factor of 1.87; and $[Yb]_{10}$ from 1.26 to 2.68, a factor of 2.12. That is, the $[Yb]_{10}$ is more variable than $[La]_{10}$ and $[Nb]_{10}$ within Mahukona lavas. During partial melting of peridotite, Yb is more compatible than La and Nb [e.g., *Salters*, 1996; *Salters and Longhi*, 1999; *Salters et al.*, 2002] (Table 5); therefore melts generated from a common peridotite should have Yb abundances less variable than La and Nb abundances [e.g., *Hanson*, 1989]. In detail, partial melts from a garnet peridotite have variable Nb abundances but relatively constant Yb abundances (Figure 8b), since Yb is buffered by garnet. Partial melts from a spinel peridotite form a convex upward trend in a Nb-Yb plot (Figure 8b).

Table 4b. Pb Isotopic Ratios in Mahukona Lavas

Sample	Group	$^{206}Pb/^{204}Pb$	2 Sigma	$^{207}Pb/^{204}Pb$	2 Sigma	$^{208}Pb/^{204}Pb$	2 Sigma
Transitional lavas							
F288HW-D18-6		18.3294	0.0024	15.4759	0.0030	38.0859	0.0100
F288HW-D18-6[a]		18.3209	0.0018	15.4653	0.0016	38.0530	0.0043
D6-R3[a]		18.3489	0.0004	15.4796	0.0004	38.1101	0.0012
D6-R6[a]		18.3360	0.0006	15.4738	0.0006	38.0884	0.0018
Tholeiitic lavas							
F288HW-D17	A	18.2787	0.0020	15.4699	0.0024	37.9541	0.0078
P5-65-1	A	18.3269	0.0023	15.4724	0.0029	37.9712	0.0096
P5-65-5	A	18.3275	0.0066	15.4686	0.0060	37.9660	0.0160
P5-72-5	A	18.3112	0.0019	15.4731	0.0024	37.9598	0.0079
P5-72-7	A	18.3207	0.0026	15.4739	0.0032	37.9652	0.0104
P5-72-8	A	18.3179	0.0026	15.4713	0.0032	37.9573	0.0105
P5-75-1	A	18.2943	0.0030	15.4707	0.0036	37.9568	0.0118
F288HW-D16-2	B	18.2931	0.0019	15.4728	0.0023	37.9667	0.0075
F288HW-D19-9	B	18.3572	0.0030	15.4783	0.0038	38.0208	0.0123
P5-65-6[a]	B	18.3222	0.0004	15.4776	0.0004	37.9511	0.0010
P5-65-7	B	18.3174	0.0020	15.4753	0.0025	37.9462	0.0082
P5-65-8B	B	18.3176	0.0026	15.4764	0.0032	37.9491	0.0105
P5-73-3	B	18.2050	0.0029	15.4646	0.0036	37.9163	0.0118
P5-73-4	B	18.1768	0.0018	15.4638	0.0023	37.9145	0.0074
P5-73-5	B	18.1753	0.0027	15.4628	0.0035	37.9124	0.0113
P5-75-4	B	18.2068	0.0016	15.4662	0.0020	37.9234	0.0066
P5-72-1	high CaO	17.9691	0.0024	15.4537	0.0030	37.7654	0.0098
P5-72-1[a]	high CaO	17.9769	0.0006	15.4514	0.0006	37.7600	0.0016
P5-72-3[a]	high CaO	17.9744	0.0004	15.4545	0.0004	37.7678	0.0012

[a] Analyses done at Florida State University.

Consequently, it is unlikely that the linear $[Nb]_{10}$-$[Yb]_{10}$ of Mahukona lavas can be explained by partial melting of a common peridotite mantle source (Figure 8). In addition, Mahukona high-CaO lavas have the lowest $[Nb]_{10}$ and highest Nb/Yb among Mahukona lavas (Figure 8c), a feature that cannot be explained by partial melting. Consequently, Mahukona lavas were derived from compositionally heterogeneous sources, an inference that is consistent with their isotopic heterogeneity (Figures 4–7).

4.2. Geochemical Variations Within Mahukona Lavas: CaO Contents

[14] Mahukona tholeiitic lavas define three distinct groups in an MgO-CaO plot (Figure 2a). At a given MgO content, the CaO range in Mahukona tholeiitic lavas is greater than that in Mauna Loa and Mauna Kea lavas. What is the origin of this variability in CaO content?

[15] Is the CaO variation a result of different magma segregation pressures? Experiments on volatile-free partial melting of garnet peridotite and the associated model calculations indicate that CaO and SiO_2 contents in partial melt decrease with increasing melting pressure [e.g., *Walter*, 1998; *Stolper et al.*, 2004]. Within Mahukona tholeiitic lavas, the high-CaO lavas have the highest CaO content and the lowest SiO_2 content at a given MgO, inconsistent with CaO variation being controlled by melting pressure.

[16] *Herzberg* [2006] and *Herzberg and Asimow* [2008] proposed that CaO content at a given MgO content distinguishes between partial melts of peridotite and garnet pyroxenite. On the basis of the partial melting experiments of *Walter* [1998], *Herzberg* [2006] showed that partial melts from peridotite have CaO contents higher than most Mauna Kea tholeiitic lavas; only the Mauna Kea CaO-K_2O-rich glasses can be explained as partial melts of peridotite (Figure 2a) [*Herzberg*, 2006]. Consequently, the relatively low CaO content in most Hawaiian tholeiitic lavas may reflect a garnet pyroxenite source [*Herzberg*, 2006]. A caveat, however, is that the degrees of partial melting in the experiments of *Walter* [1998] are large (>10%), and lower degree partial melting of peridotite may lead to lower CaO content (e.g., the model lines given by *Stolper et al.* [2004, Figure 13]). But recent partial melting experiments revealed that low-degree partial melts of garnet peridotite have high CaO contents [*Davis et al.*, 2008; *Balta et al.*, 2008]. For example, *Davis et al.* [2008] reported that at very low degree of partial melting, partial melt of a garnet peridotite has [CaO] = 12.1% and

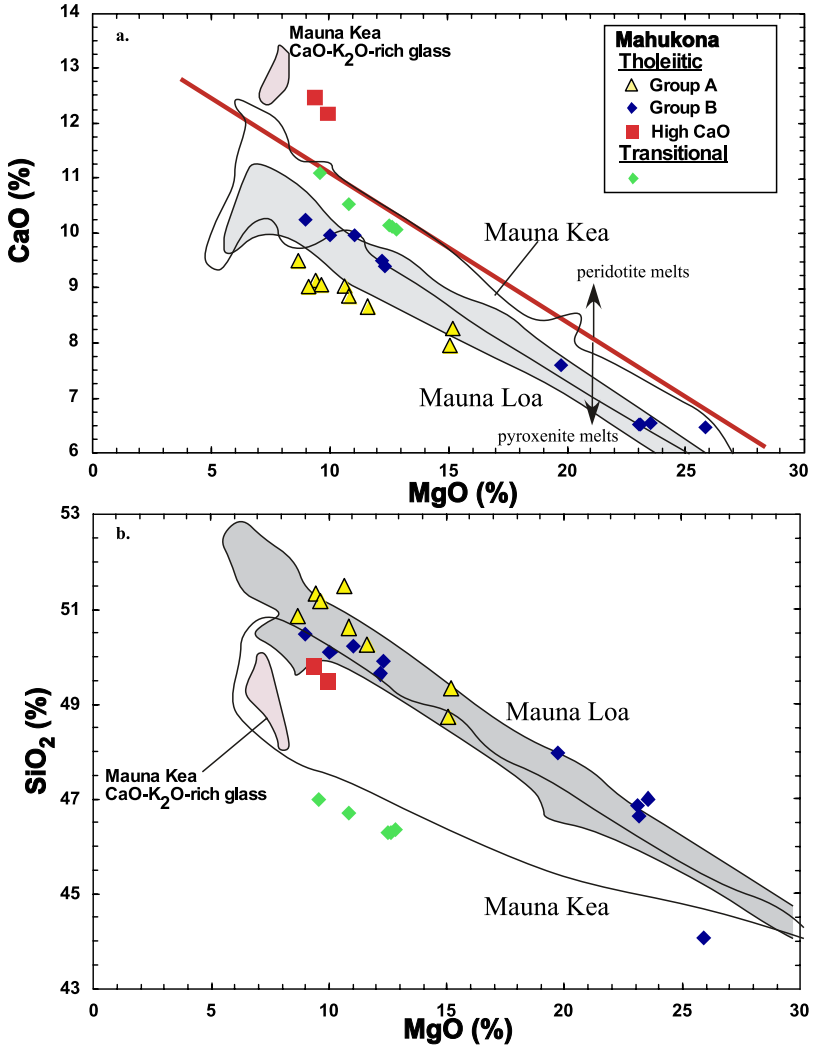

Figure 2. MgO versus (a) CaO and (b) SiO_2 (all in wt %) for Mahukona lavas. Fields for shield stage tholeiitic lavas from Mauna Loa and Mauna Kea are shown for comparison. The red line separating the partial melts of peridotite from partial melts from garnet pyroxenite is taken from *Herzberg* [2006]. Data sources are as follows: Mauna Loa, *Garcia et al.* [1995a], *Rhodes* [1995, 1996], *Rhodes and Hart* [1995], and *Rhodes and Vollinger* [2004]; Mauna Kea, *Rhodes* [1996], *Rhodes and Vollinger* [2004], and *Stolper et al.* [2004].

[MgO] = 17.0%, a result that is consistent with the *Herzberg*'s [2006] model but inconsistent with the model calculation using the algorithm of *Longhi* [2002] presented by *Stolper et al.* [2004, Figure 13]. On the other hand, partial melts from some silica-undersaturated garnet pyroxenites could yield high CaO contents [e.g., *Hirschmann et al.*, 2003; *Kogiso et al.*, 2003; *Keshav et al.*, 2004]. However, *Herzberg and Asimow* [2008] argued that the starting garnet pyroxenites used in these experiments have compositions similar to high-pressure crystal cumulates [e.g., *Frey*, 1980; *Keshav et al.*, 2007]. Therefore, these experimental results may not be applicable to mantle melting. A conservative inference is that, for Hawaiian shield tholeiitic lavas, low CaO contents may not necessarily be an indicator of a garnet pyroxenite origin, but high CaO contents are indicative of a peridotite source. That is, on the basis of their high CaO contents, we infer that Mahukona high-CaO lavas and Mauna Kea CaO-K_2O-rich lavas originated from peridotite, with minimal contribution from garnet pyroxenite. The peridotite origin of Mahukona high-CaO lavas is also consistent with our unpublished Fe/Mn data (S. Huang and M. Humayun, unpublished data, 2009). Partial melts from olivine-free garnet pyroxenite tend to have higher Fe/Mn than partial melts from peridotite [*Humayun et al.*, 2004; *Sobolev et al.*, 2007], and Mahukona high-CaO lavas have lower Fe/Mn than other Mahukona lavas

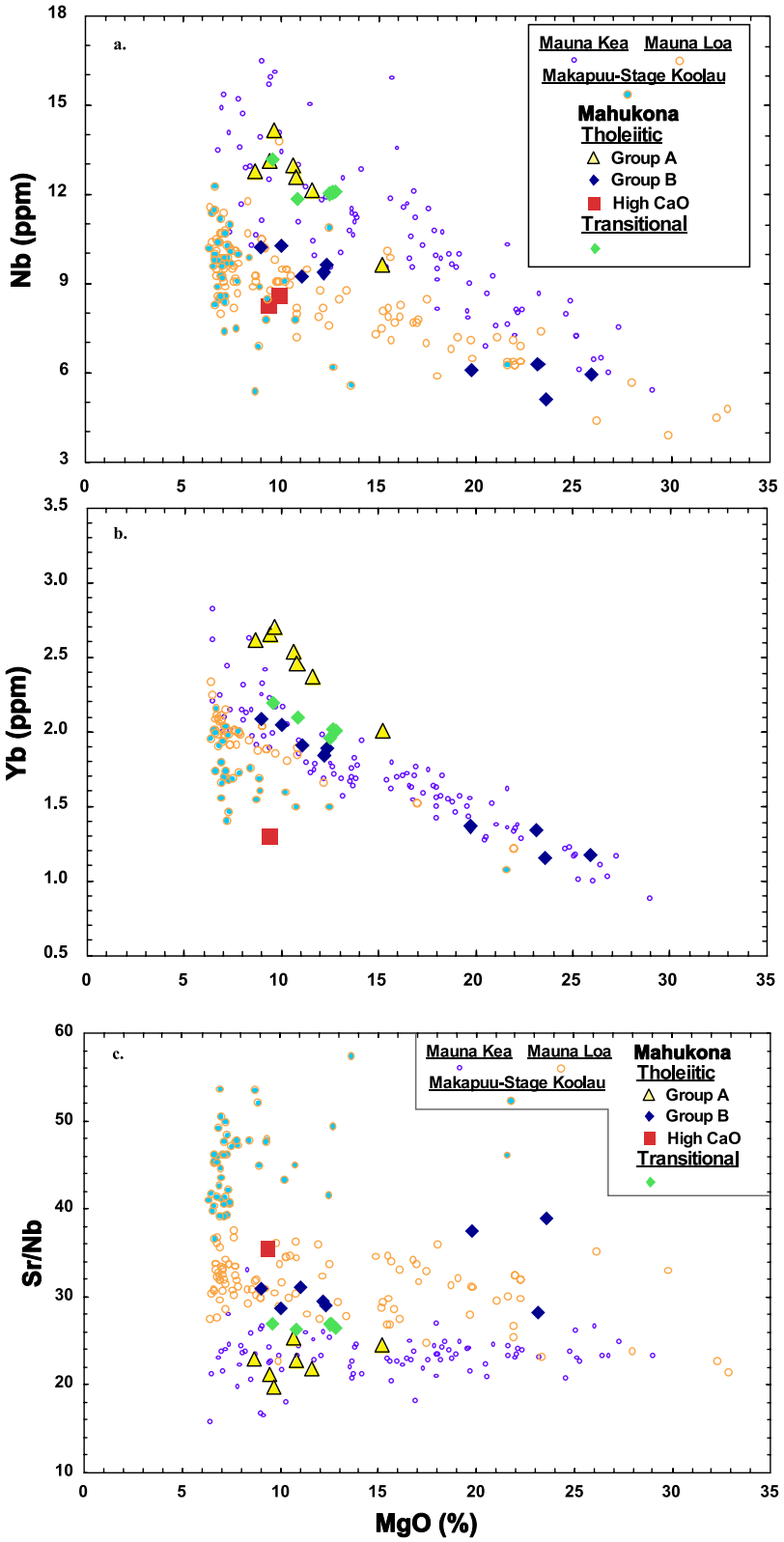

Figure 3. MgO (in wt %) versus (a) Nb and (b) Yb (in ppm) and (c) Sr/Nb for Mahukona lavas. Shield stage tholeiitic lavas from Makapuu-stage Koolau, Mauna Kea, and Mauna Loa are shown for comparison. Data sources are as follows: Makapuu-stage Koolau, *Frey et al.* [1994]; Mauna Kea, *Rhodes and Vollinger* [2004] and *Huang and Frey* [2003]; Mauna Loa, *Garcia et al.* [1995a], *Rhodes* [1995, 1996], *Rhodes and Hart* [1995], and *Rhodes and Vollinger* [2004].

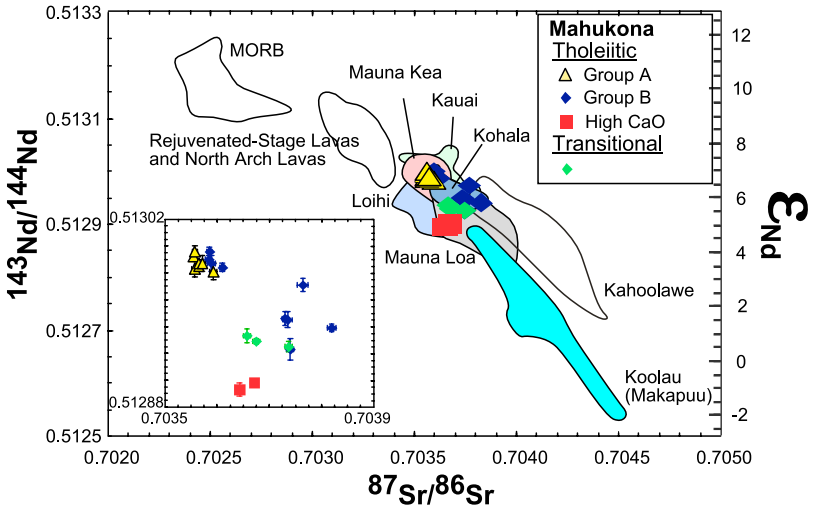

Figure 4. $^{87}Sr/^{86}Sr$ versus $^{143}Nd/^{144}Nd$ for Mahukona lavas. Fields for Hawaiian shields are shown for comparison. The inset shows a blow up of Mahukona data, along with the 2σ error bars. Data sources are as follows: Kahoolawe lavas, *West et al.* [1987] and *Huang et al.* [2005b]; Koolau (Makapuu), *Roden et al.* [1984, 1994]; Mauna Kea, *Lassiter et al.* [1996] and *Bryce et al.* [2005]; Mauna Loa, *Cohen et al.* [1996] and *Kurz et al.* [1995]; Kauai, *Mukhopadhyay et al.* [2003]; Loihi, *Garcia et al.* [1993, 1995b, 1998]; Kohala, *Hofmann et al.* [1987]; rejuvenated stage lavas, *Stille et al.* [1983], *Roden et al.* [1984], *Chen and Frey* [1985], *Tatsumoto et al.* [1987], *West et al.* [1987], *Frey et al.* [2000], and *Lassiter et al.* [2000]; EPR MORB, *Niu et al.* [1999], *Regelous et al.* [1999], and *Castillo et al.* [2000].

(S. Huang and M. Humayun, unpublished data, 2009).

[17] Since Yb and Ca (as CaO) are compatible during partial melting of garnet pyroxenite (eclogite) [e.g., *Pertermann et al.*, 2004], partial melts of garnet pyroxenite, such as dacite, have low Yb and CaO abundances relative to partial melts of peridotite. Figure 9 shows that at a given $[Yb]_{10}$, $[CaO]_{10}$ decreases in shield stage lavas from

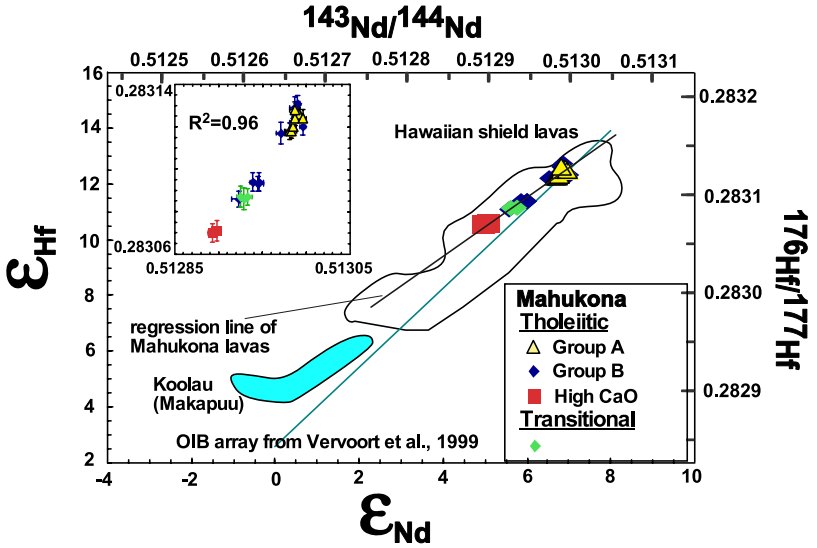

Figure 5. Plot of $^{143}Nd/^{144}Nd$ versus $^{176}Hf/^{177}Hf$ for Mahukona lavas. Fields for Hawaiian shields are shown for comparison. The inset shows a blow up of Mahukona data. The 2σ error bars and linear correlation coefficient for Mahukona lavas are also shown in the inset. $\varepsilon_{Hf} = (((^{176}Hf/^{177}Hf)_{sample}/(^{176}Hf/^{177}Hf)_{CHUR} - 1) \times 10000$ and $\varepsilon_{Nd} = (((^{143}Nd/^{144}Nd)_{sample}/(^{143}Nd/^{144}Nd)_{CHUR} - 1) \times 10000$ with $(^{176}Hf/^{177}Hf)_{CHUR} = 0.282772$ [*Blichert-Toft and Albarède*, 1997] and $(^{143}Nd/^{144}Nd)_{CHUR} = 0.512638$. The fields for Makapuu-stage Koolau lavas and other Hawaiian shield lavas [*Blichert-Toft et al.*, 1999], as well as the OIB array [*Vervoort et al.*, 1999], are shown for comparison.

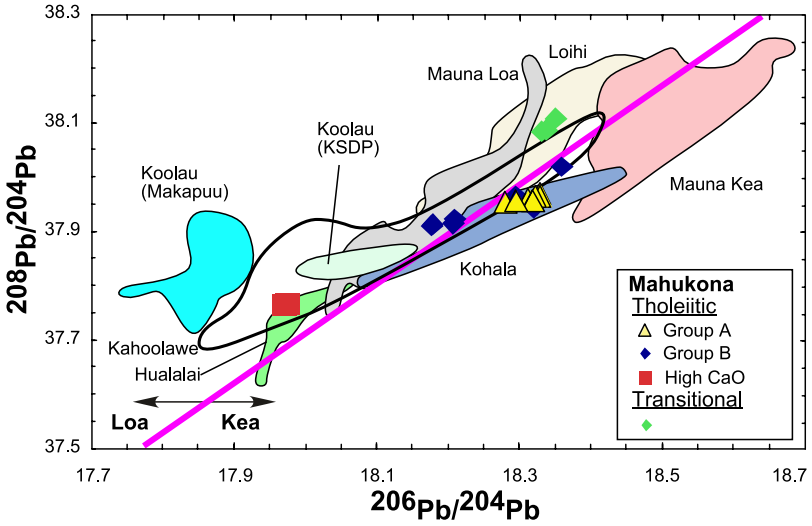

Figure 6. Plot of $^{208}Pb/^{204}Pb$ versus $^{206}Pb/^{204}Pb$ for Mahukona lavas. Fields for Hawaiian shields are shown for comparison. The 2σ error bars for Mahukona lavas are smaller than the symbols. The Loa-Kea dividing line is from *Abouchami et al.* [2005]. Data sources are as follows: Makapuu-stage Koolau, *Roden et al.* [1994] and *Abouchami et al.* [2005]; Koolau (KSDP), *Fekiacova et al.* [2007]; Kahoolawe, *West et al.* [1987], *Abouchami et al.* [2005], and *Huang et al.* [2005b]; Mauna Loa, *Kurz et al.* [1995], *Cohen et al.* [1996], and *Abouchami et al.* [2000]; Loihi, *Garcia et al.* [1993, 1995b, 1998]; Hualalai, *Cousens et al.* [2003]; Mauna Kea, *Abouchami et al.* [2000], *Blichert-Toft et al.* [2003], and *Eisele et al.* [2003]; Kohala, *Abouchami et al.* [2005].

Mauna Kea to Mauna Loa to Makapuu-stage Koolau; also, the Makapuu-stage Koolau lavas range to the lowest $[Yb]_{10}$. These observations can be explained as a mixing trend between partial melts of peridotite and partial melts of garnet pyroxenite, with Makapuu-stage Koolau lavas containing the largest amount of partial melts derived from silica-saturated garnet pyroxenite [e.g., *Hauri*, 1996; *Lassiter and Hauri*, 1998; *Huang and Frey*, 2005; *Sobolev et al.*, 2005, 2007; *Fekiacova et al.*, 2007; *Huang et al.*, 2007]. In contrast, Mauna Kea shield and postshield tholeiitic lavas form a negative trend in a $[Yb]_{10}$-$[CaO]_{10}$ plot, and Mahukona lavas overlap with the Mauna Kea trend in this plot (Figure 9). This negative $[Yb]_{10}$-$[CaO]_{10}$ trend cannot be explained as a result of sampling partial melts of garnet pyroxenite (eclogite). In addition, as discussed above, on

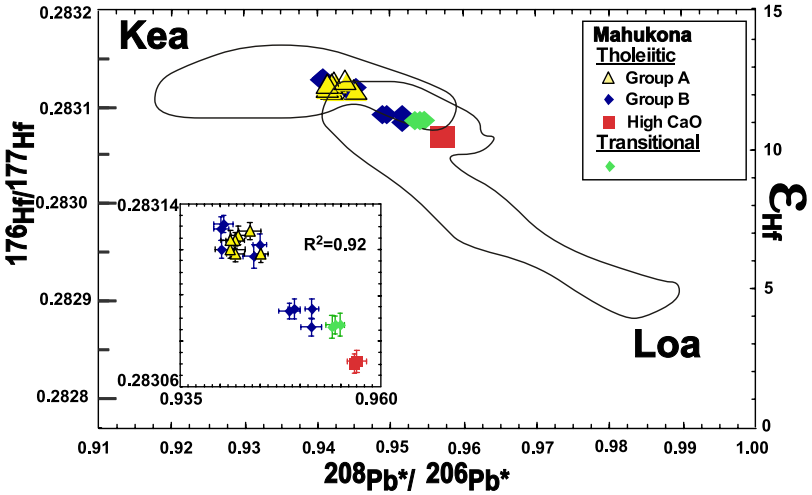

Figure 7. Plot of $^{208}Pb/^{206}Pb^*$ versus $^{176}Hf/^{177}Hf$ for Mahukona lavas. Fields for Loa and Kea trend lavas are from *Huang et al.* [2005b]. Inset is a blow up of Mahukona data. The 2σ error bars and linear correlation coefficient for Mahukona lavas also are shown in the inset.

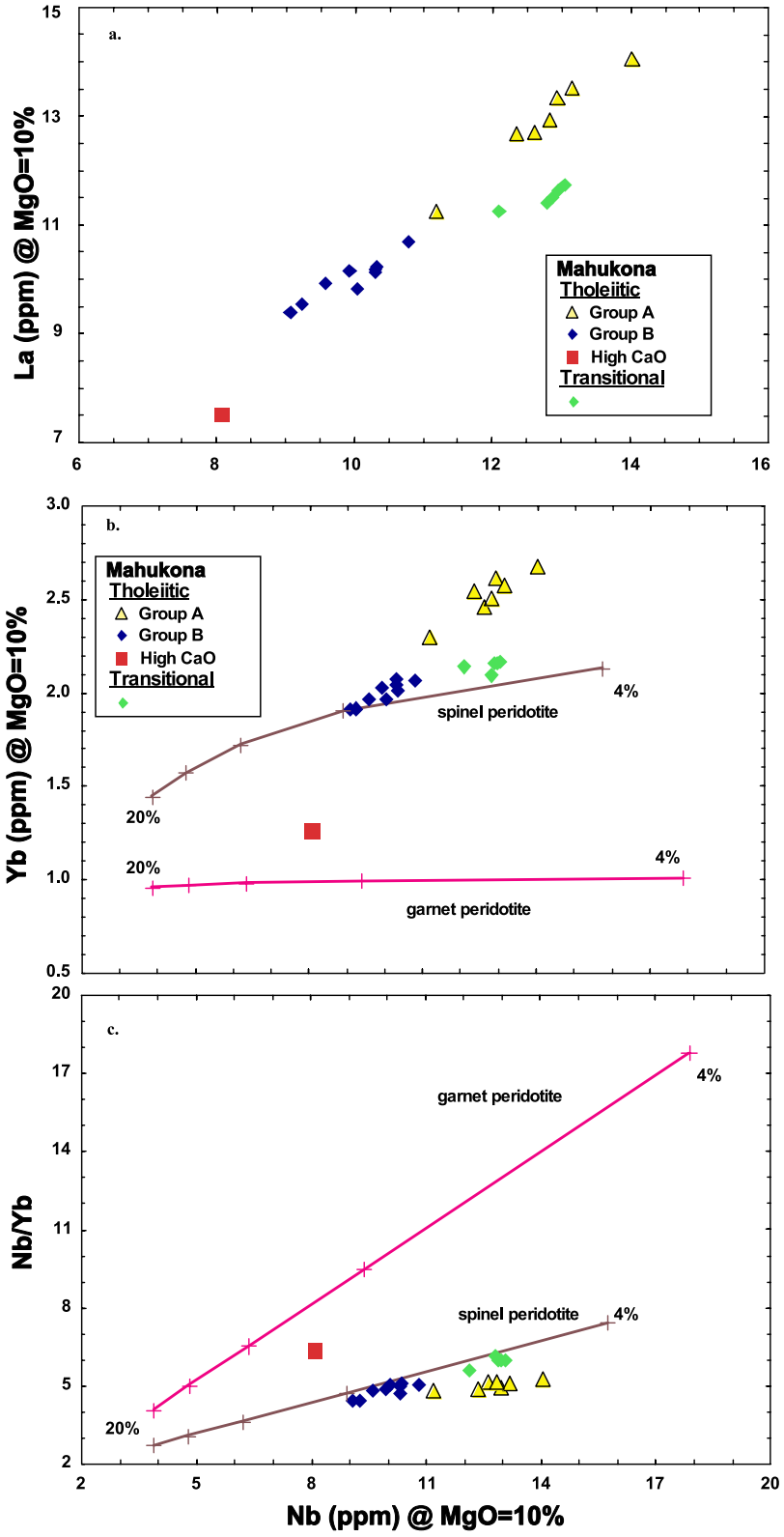

Figure 8. Nb versus (a) La, (b) Yb (all in ppm, adjusted to MgO = 10%), and (c) Nb/Yb for Mahukona lavas. Two model lines of the partial melts of spinel peridotite and garnet peridotite are shown for comparison. The melting increment is 4%, with the maximum and minimum melting extents labeled at both ends. Model parameters are in Table 5.

Table 5. Input Parameters for Melting Model

	Olivine	Orthopyroxene	Clinopyroxene	Spinel	Garnet	Nb (ppm)	Yb (ppm)
			Source Mode[a]				
Garnet peridotite	0.53	0.04	0.38	0	0.05	0.78	0.33
Spinel peridotite	0.53	0.2	0.25	0.02	0	0.78	0.33
			Melting Reaction[a]				
Garnet peridotite	0.05	−0.49	1.31	0	0.13		
Spinel peridotite	0.375	−0.5	1.125	0	0		
			Partition Coefficients				
Garnet peridotite							
Nb	0	0.00022[b]	0.008[c]		0.023[c]		
La	0	0.00001[b]	0.008[c,e]		0.023[c,e]		
Yb	0	0.02[b]	0.174[c]		5.17[c]		
Spinel peridotite							
Nb	0	0.0013[b]	0.045[d]	0			
La	0	0.00008[b]	0.045[d,e]	0			
Yb	0	0.0569[b]	0.503[d]	0			

[a] From *Salters* [1996, Table 2].
[b] Calculated using $K_d^{OPX/CPX}$ values of sample 2905 from *Eggins et al.* [1998].
[c] From *Salters and Longhi* [1999], sample TM 694-6 (2.8GPa and 1537°C).
[d] From *Salters and Longhi* [1999], sample TM 1094-9 (1.5GPa and 1502°C).
[e] $Kd_{La}^{CPX/melt} = Kd_{Nb}^{CPX/melt}$ and $Kd_{La}^{Grt/melt} = Kd_{Nb}^{Grt/melt}$ are assumed.

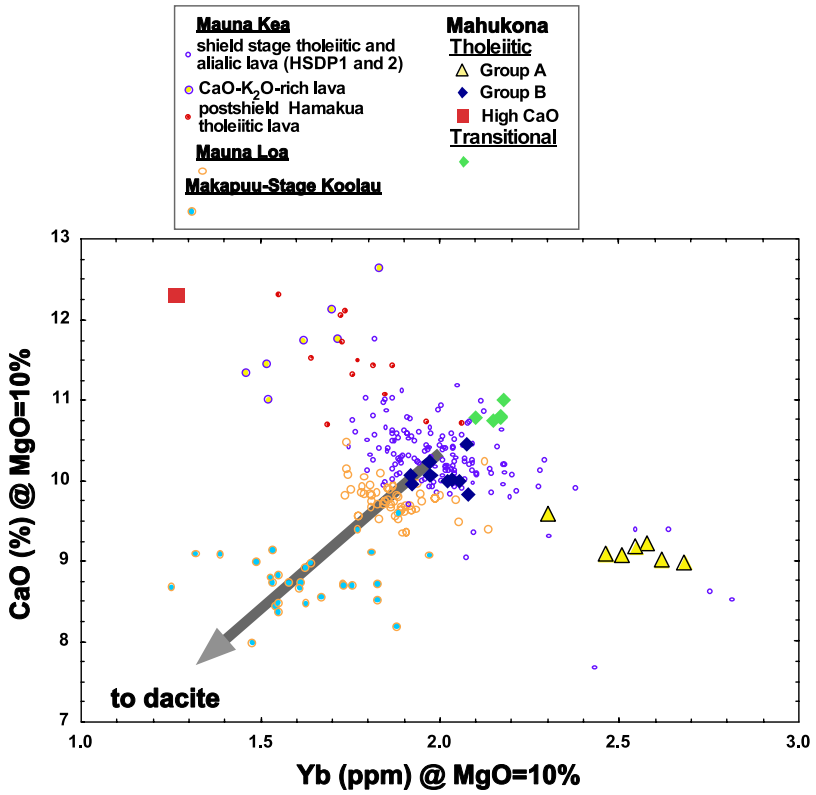

Figure 9. Yb (in ppm) versus CaO (in wt %) (adjusted to MgO = 10%) for Mahukona lavas. Lavas from Makapuu-stage Koolau, Mauna Kea, and Mauna Loa are shown for comparison. Dacite magmas have low CaO and Yb contents; consequently, mixing with dacite results in lower CaO and Yb contents as indicated by the arrow. For data sources see captions of Figures 2 and 3, with data of Mauna Kea postshield Hamakua tholeiitic lavas from *Frey et al.* [1991].

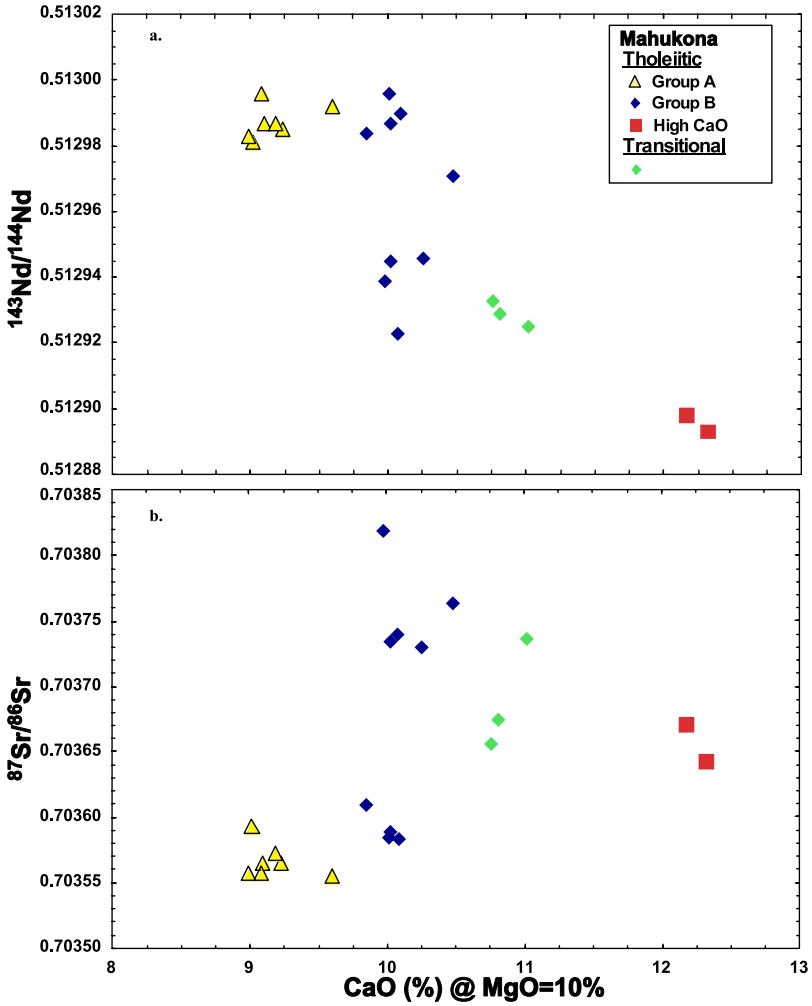

Figure 10. CaO (in wt %, adjusted to MgO = 10%) versus (a) Nd and (b) Sr isotopic ratios for Mahukona lavas.

the basis of trace element abundances, the large range in $[Yb]_{10}$ of Mahukona lavas cannot be generated by partial melting of a common peridotite (Figure 8). Therefore, we infer that the negative $[Yb]_{10}$-$[CaO]_{10}$ trend of Mahukona lavas is a magma mixing trend. Consistent with this inference, among Mahukona lavas $[CaO]_{10}$ is broadly correlated with $^{143}Nd/^{144}Nd$ (Figure 10).

[18] Since carbonatites are characterized by high CaO content (>30%) [e.g., *Nelson et al.*, 1988; *Le Roex and Lanyon*, 1998; *Hoernle et al.*, 2002], could the CaO variation within Mahukona lavas represent mixing between partial melt of peridotite and carbonatite melt? On the basis of incompatible element abundances and radiogenic isotopic ratios in Mahukona lavas, the answer appears to be no. First, it is well established that carbonatites have high abundances of most incompatible elements. For example, Yb abundances in carbonatites in general are greater than 3 ppm [e.g., *Nelson et al.*, 1988; *Le Roex and Lanyon*, 1998; *Hoernle et al.*, 2002]. In contrast, Mahukona high-CaO lavas have the lowest incompatible element abundances among Mahukona lavas (Figures 3, 8, and 9), inconsistent with varying amounts of carbonatite contribution. This argument may be weakened by the argument that carbonatites generated at high pressure may be characterized by low Yb abundances because of a high proportion of residual garnet [e.g., *Dasgupta et al.*, 2009]. Also, most carbonatites are strongly depleted in high field strength elements (HSFE) [e.g., *Nelson et al.*, 1988; *Le Roex and Lanyon*, 1998; *Hoernle et al.*, 2002]; however, Mahukona lavas do not have relative depletion in HSFE (Figure 11).

[19] Second, *Bizimis et al.* [2003] argued that a carbonatite melt has relatively high Lu/Hf; consequently, with time the typically observed positive

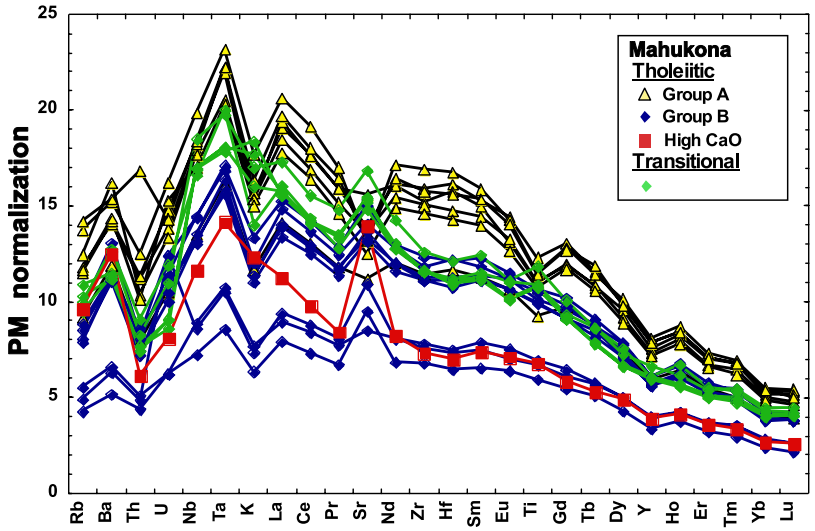

Figure 11. Primitive mantle normalized trace element abundances of Mahukona lavas. Primitive mantle values are from *Hofmann* [1988].

correlation between $^{143}Nd/^{144}Nd$ and $^{176}Hf/^{177}Hf$ will be perturbed but without affecting the typical negative correlation between $^{87}Sr/^{86}Sr$ and $^{143}Nd/^{144}Nd$. However, within Mahukona lavas, $^{143}Nd/^{144}Nd$ is highly correlated with $^{176}Hf/^{177}Hf$ (Figure 5), but decoupled from $^{87}Sr/^{86}Sr$ (Figure 4).

[20] Consequently, it is unlikely that the CaO variation within Mahukona lavas reflects varying amounts of carbonatite. Nevertheless, it is likely that CO_2 or carbonate was important during the petrogenesis of the Mahukona shield stage lavas that have relatively high CaO and low SiO_2 contents. A trend of increasing CaO and decreasing SiO_2 contents is also defined by postshield stage lavas erupted at Mauna Kea volcano [*Yang et al.*, 1996] and the rejuvenated stage Honolulu Volcanics erupted at Koolau volcano [*Clague and Frey*, 1982]. On the basis of experimental studies, a varying abundance of CO_2 in the magma source regions can explain such trends [e.g., *Frey and Rhodes*, 1993].

4.3. Geochemical Variations Within Mahukona Lavas: Sr Isotopic Ratios

[21] The large isotopic variations of Hawaiian shield lavas reflect geochemical heterogeneity within the Hawaiian plume, which is interpreted to result from sampling recycled ancient oceanic crust (including sediments) [e.g., *Lassiter and Hauri*, 1998; *Blichert-Toft et al.*, 1999]. Radiogenic isotopic ratios of Mahukona lavas do not define end-members in any isotopic plots (Figures 4–7). It is therefore unlikely that Mahukona lavas provide new constraints on the origin of the Hawaiian isotopic end-members, such as the Makapuu-stage Koolau and the Kea end-members [e.g., *Hauri*, 1996]. However, an important characteristic of Mahukona lavas is the decoupling of $^{87}Sr/^{86}Sr$ from Nd, Hf and Pb isotopic ratios. Despite excellent correlations between Nd-Hf-Pb isotopic ratios, $^{87}Sr/^{86}Sr$ does not correlate with these other radiogenic isotopic systems in Mahukona lavas (Figures 4, 5, and 7); consequently, a process is required to explain the $^{87}Sr/^{86}Sr$ and Sr abundances of Mahukona lavas. We note that $^{87}Sr/^{86}Sr$ is highly correlated with trace element abundance ratios involving Sr, such as Sr/Ce, Ba/Sr and Rb/Sr (Figure 12). The negative $^{87}Sr/^{86}Sr$-Rb/Sr trend formed by Mahukona lavas (Figure 12c) cannot be the result of in situ radiogenic ingrowth of ^{87}Sr, which generates a positive trend in an $^{87}Sr/^{86}Sr$-Rb/Sr plot. The linear trends of $^{87}Sr/^{86}Sr$ versus Sr/Ce, Ba/Sr and Rb/Sr defined by Mahukona lavas are best explained as binary mixing lines between a low-$^{87}Sr/^{86}Sr$, low-Sr/Ce, high-Ba/Sr and high-Rb/Sr end-member overlapping with the Kilauea field and a high-$^{87}Sr/^{86}Sr$, high-Sr/Ce, low-Ba/Sr and low-Rb/Sr end-member. Consequently, a source component with $^{87}Sr/^{86}Sr > 0.7038$, Sr/Ce > 18, Ba/Sr < 0.15 and Rb/Sr < 0.01, i.e., a Sr-rich component, contributed to Mahukona lavas. It is inferred that this Sr-rich component adds negligible amounts of Nd-Hf-Pb to the Mahukona source. Accordingly, it affects only $^{87}Sr/^{86}Sr$ and abundance ratios involving Sr, but it does not affect the highly correlated $^{176}Hf/^{177}Hf$, $^{143}Nd/^{144}Nd$ and $^{208}Pb^*/^{206}Pb^*$ in Mahukona lavas (Figures 5 and 7).

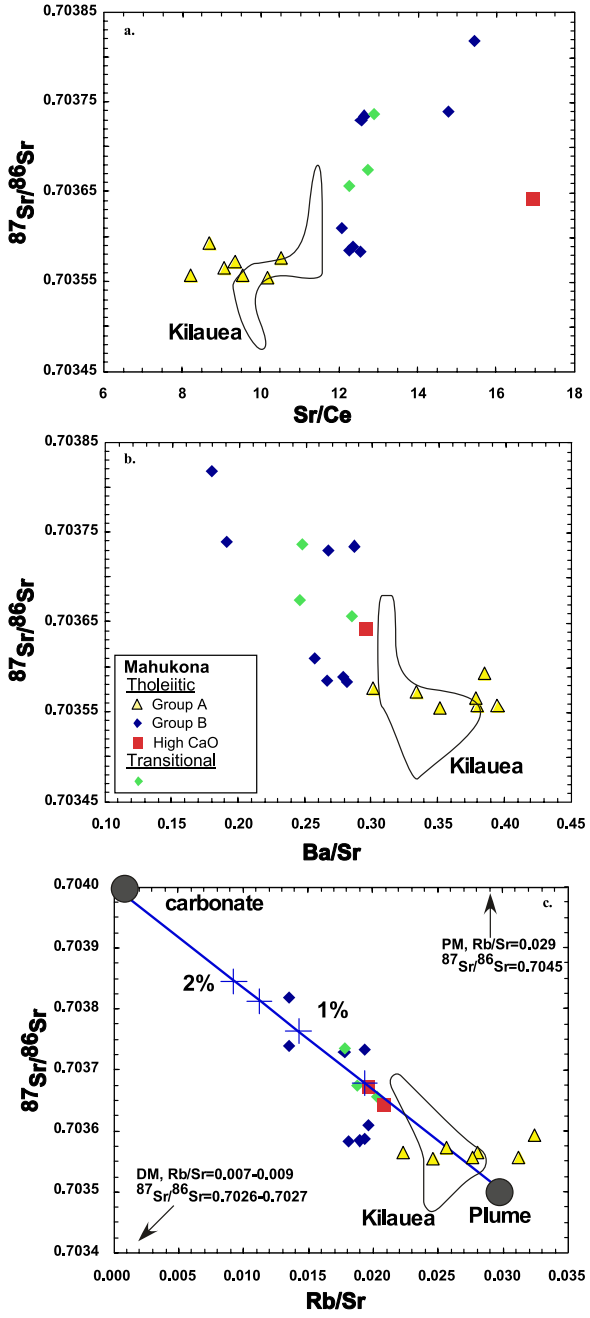

Figure 12. (a) Sr/Ce, (b) Ba/Sr, and (c) Rb/Sr versus $^{87}Sr/^{86}Sr$ for Mahukona lavas. Kilauea glasses [*Pietruszka and Garcia*, 1999] are plotted for comparison. Primitive mantle (PM) and depleted mantle (DM) [from *Hofmann*, 1988; *Salters and Stracke*, 2004; *Workman and Hart*, 2005] are plotted in Figure 12c for comparison. A mixing line between a plume component ([Sr] = 18.2 ppm, Rb/Sr = 0.03, and $^{87}Sr/^{86}Sr$ = 0.7035) and a carbonate component ([Sr] = 2000 ppm, Rb/Sr = 0, and $^{87}Sr/^{86}Sr$ = 0.7040) is shown in Figure 12c. The plume component is assumed to have primitive mantle-like Sr abundance and Rb/Sr [*Hofmann*, 1988] and the lowest $^{87}Sr/^{86}Sr$ in Kilauea lavas [*Pietruszka and Garcia*, 1999].

This Sr-rich component is not primitive or depleted mantle because these two reservoirs do not plot on the negative $^{87}Sr/^{86}Sr$-Rb/Sr trend defined by Mahukona lavas (Figure 12c). What then is its origin?

[22] Two types of Sr-rich component have been proposed for Hawaiian shield lavas: recycled ancient plagioclase-rich gabbroic crust [*Hofmann and Jochum*, 1996; *Sobolev et al.*, 2000; *Huang et al.*, 2005b] and recycled ancient carbonate-rich sediments [*Huang and Frey*, 2005]. Since plagioclase-rich gabbroic crust is characterized by very low Rb/Sr, the $^{87}Sr/^{86}Sr$ of ancient gabbroic crust does not change significantly with time and hence will be relatively unradiogenic even at present [e.g., *Zimmer et al.*, 1995]. In contrast, authigenic marine sediments inherit $^{87}Sr/^{86}Sr$ from seawater, and even at 2 Ga seawater $^{87}Sr/^{86}Sr$ was more radiogenic (~0.704 [*Ray et al.*, 2002; *Shields and Veizer*, 2002]) than most mantle end-members because of riverine input of dissolved crustal Sr. We thus suggest that the Sr-rich source component sampled by Mahukona lavas is recycled ancient carbonate-rich sediment. The $^{87}Sr/^{86}Sr$ and Rb/Sr variation in Mahukona lavas can be explained by adding up to 1.5% recycled ancient carbonate-rich sediment ($^{87}Sr/^{86}Sr$ = 0.704, Rb/Sr = 0, which corresponds to carbonates with an age of 2.0 Ga [*Shields and Veizer*, 2002]) into a Kilauea-like mantle source (Figure 12c).

[23] *Frey et al.* [1994] noted that Hawaiian shield tholeiitic lavas show a broad positive trend in a Sr/Nb-La/Nb plot, with Makapuu-stage Koolau lavas having the highest Sr/Nb and La/Nb (Figure 13). In conjunction with their high $^{87}Sr/^{86}Sr$ and low Th/La, *Huang and Frey* [2005] proposed that a recycled ancient carbonate- and phosphate-rich sedimentary source component contributed to Koolau lavas. Further, *Huang and Frey* [2005] concluded that the high La/Nb and low Th/La in Makapuu-stage Koolau lavas result from REE enrichment. Since marine sediments can be mixtures of several lithological end-members, we infer that the REE enrichment in the Makapuu-stage Koolau lavas originated from a REE-rich phosphate-bearing carbonate component in the recycled ancient sediment [e.g., *Plank and Langmuir*, 1998, Figure 6]. On the other hand, because marine carbonates have very low abundances of La and Nb, we infer that the Sr/Nb variation within Hawaiian shield lavas results from variable amounts of carbonate component (Figure 13). Mahukona lavas have variable Sr/Nb (20–40) but relatively

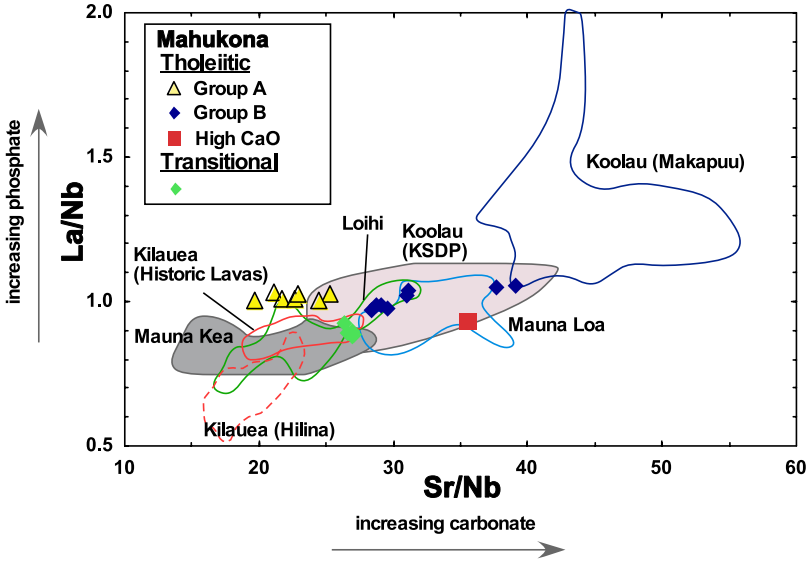

Figure 13. Sr/Nb versus La/Nb for Mahukona lavas. Fields for Koolau (Makapuu stage and KSDP), Mauna Loa, Mauna Kea, Loihi, and Kilauea (Hilina and historical lavas) are shown for comparison. Increasing amounts of recycled ancient carbonate component result in increasing Sr/Nb, and increasing amounts of recycled ancient phosphate component result in increasing La/Nb. Modified from *Huang and Frey* [2003].

constant La/Nb (0.98 ± 0.05, 1σ) (Figure 13), implying that the recycled ancient carbonate-rich sedimentary component sampled by Mahukona lavas did not contain significant amounts of REE-rich phosphate.

[24] We show that up to 1.5% ancient carbonate is required to explain the $^{87}Sr/^{86}Sr$-Rb/Sr trend of Mahukona lavas (Figure 12c). Assuming the Kilauea-like mantle source has 3.54% CaO, the primitive upper mantle value estimated by *McDonough and Sun* [1995], adding 1.5% ancient carbonate will increase the CaO content by ~20%, which can significantly increase the (clinopyroxene+garnet)/(orthopyroxene+olivine) ratio in the source assuming that carbonate sediment reacted with peridotite. Could the CaO variation in Mahukona lavas be explained by adding various amounts of recycled ancient carbonate? $[CaO]_{10}$ does not correlate with $^{87}Sr/^{86}Sr$, an indicator of the amount of recycled ancient carbonate (Figure 10b). Especially, Mahukona Group B tholeiitic lavas show large ranges of $^{87}Sr/^{86}Sr$, Rb/Sr, Sr/Ce and Ba/Sr (Figure 12), but they have relatively constant $[CaO]_{10}$ (Figure 10b). How can this apparent inconsistency be reconciled?

[25] Calcium (as CaO) is a major constituent of garnet and clinopyroxene. During partial melting of garnet peridotite, garnet and clinopyroxene are preferentially melted and the CaO content in partial melt is controlled by the amount of garnet and clinopyroxene entering into the liquid phase [e.g., *Walter*, 1998]. Since the partial melting reaction is mostly controlled by pressure and temperature, the proportions of garnet and clinopyroxene entering into the liquid phase are determined by pressure and temperature, but not the (clinopyroxene+garnet)/(orthopyroxene+olivine) ratio of the starting peridotite. Since the CaO content in partial melt is not sensitive to either the CaO content and the (clinopyroxene+garnet)/(orthopyroxene+olivine) ratio in the starting peridotite, we conclude that variable amounts of ancient recycled carbonate controlled $^{87}Sr/^{86}Sr$, Rb/Sr, Sr/Ce and Ba/Sr, but did not control the variable CaO contents of Mahukona lavas.

4.4. Carbonate-Rich Sediments in the Hawaiian Plume: Evidence From Rb/Sr and $^{87}Sr/^{86}Sr$

[26] One of the most striking geochemical features of Mahukona lavas is their negative $^{87}Sr/^{86}Sr$-Rb/Sr trend (Figure 12c), which we used to argue that Mahukona lavas sampled a recycled ancient carbonate-rich sedimentary component. When extended to other Hawaiian shields, a negative $^{87}Sr/^{86}Sr$-Rb/Sr correlation can also be inferred. For example, Hawaiian shields exhibit large $^{87}Sr/^{86}Sr$ variation, with Makapuu-stage Koolau lavas having the most radiogenic $^{87}Sr/^{86}Sr$ among Hawaiian shield lavas (Figure 4) [*Roden et al.*, 1994]. Because Rb is sensitive to postmagmatic alteration processes [e.g., *Roden et al.*, 1994;

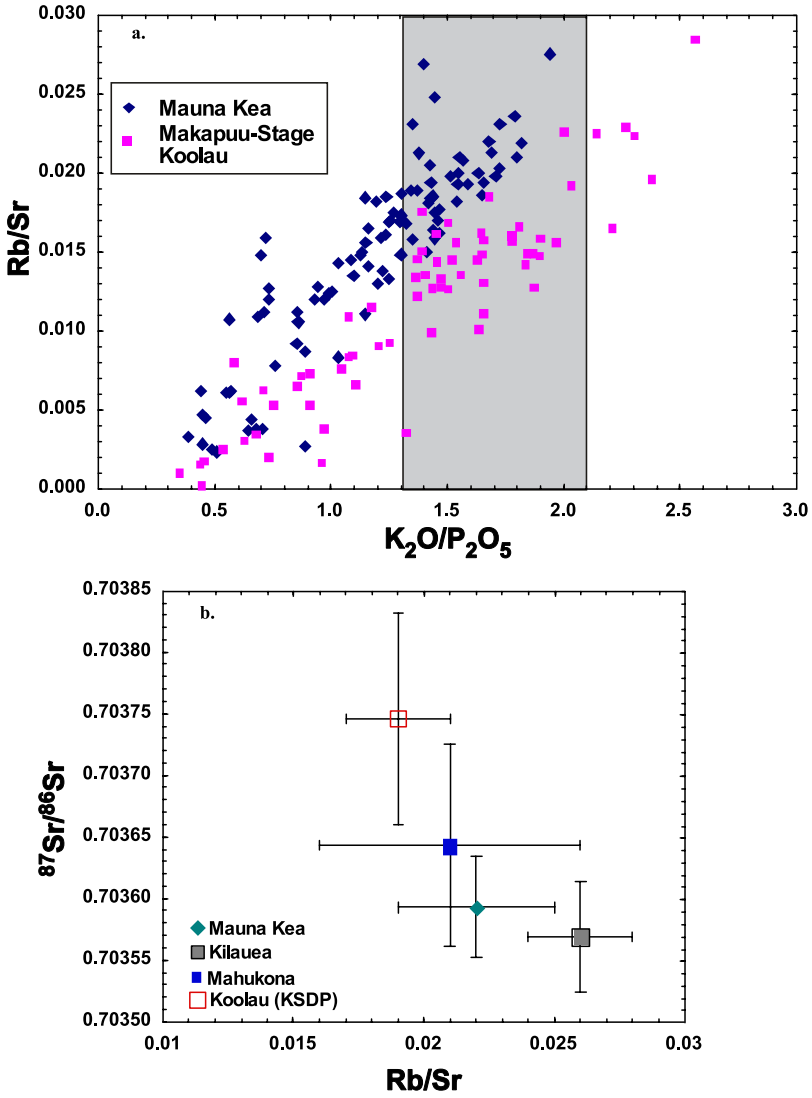

Figure 14. (a) K_2O/P_2O_5 versus Rb/Sr for Mauna Kea and Makapuu-stage Koolau lavas showing the systematically higher Rb/Sr in Mauna Kea lavas. The gray area shows the K_2O/P_2O_5 range in fresh Kilauea glasses. Data are from *Frey et al.* [1994], *Garcia et al.* [2000], *Quane et al.* [2000], *Huang and Frey* [2003], and *Rhodes and Vollinger* [2004]. (b) Average Rb/Sr versus $^{87}Sr/^{86}Sr$ with 1 standard deviation bars in several Hawaiian shields. The average Rb/Sr in KSDP of Koolau, Kilauea, and Mauna Kea are estimated using only glass data to avoid alteration effects on Rb. Note that there is no glass associated with Makapuu-stage Koolau; hence, this volcanic section is not included in this plot. Data sources are as follows: Koolau (KSDP) data are from *Haskins and Garcia* [2004] and *Fekiacova et al.* [2007]; Kilauea data are from *Pietruszka and Garcia* [1999]; and Mauna Kea data are from *Lassiter et al.* [1996], *Bryce et al.* [2005], and M. Baker (unpublished LA-ICP-MS data, 2009).

Huang and Frey, 2003], Rb/Sr ratios are affected by alteration. Since K and Rb are geochemically similar, we use K_2O/P_2O_5 as an alteration index in Hawaiian lavas [e.g., *Huang and Frey*, 2003; *Huang et al.*, 2007]. Unaltered glasses from Kilauea have $1.3 < K_2O/P_2O_5 < 2.1$ [*Garcia et al.*, 2000; *Quane et al.*, 2000]. In a K_2O/P_2O_5-Rb/Sr plot, Mauna Kea and Makapuu-stage Koolau lavas form two subparallel positive trends (Figure 14a), implying mobility of K and Rb during alteration. However, at a given K_2O/P_2O_5, Mauna Kea lavas have higher Rb/Sr than Makapuu-stage Koolau lavas, implying that the higher Rb/Sr in Mauna Kea lavas relative to lavas forming the Makapuu stage of Koolau volcano is a magmatic feature. We infer that the source of Mauna Kea lavas had higher Rb/Sr than the source of Makapuu-stage Koolau lavas. That is, the intershield geochemical heterogeneity between Mauna Kea and Makapuu-

stage Koolau is more radiogenic $^{87}Sr/^{86}Sr$ coupled with lower Rb/Sr (Figures 4 and 14a).

[27] This negative Rb/Sr-$^{87}Sr/^{86}Sr$ intershield correlation in Hawaiian shields is better shown in Figure 14b. The mobility of K and Rb caused by alteration in Hawaiian glasses is minimal; consequently, Rb/Sr in glasses represents their magmatic values. In Figure 14b, the average Rb/Sr of glasses from several Hawaiian shields is negatively correlated with their average $^{87}Sr/^{86}Sr$. Therefore, we deduce that a recycled ancient carbonate-rich sedimentary source component is important in the Hawaiian plume.

[28] A role for carbonate in the Hawaiian plume is also inferred from Hawaiian rejuvenated stage lavas. On the basis of distinctive trace element characteristics, such as high and variable Ba/Th and Sr/Ce, *Dixon et al.* [2008] argued that the mantle source of rejuvenated stage lavas from Niihau, Hawaii, was metasomatized by carbonatite melt (<0.2%), which originated from the carbonate in the Hawaiian plume. Thus, carbonates have been proposed to play an important role in the petrogenesis of Hawaiian lavas from different growth stages: the shield stage at Koolau and Mahukona [*Huang and Frey*, 2005; this study], the postshield stage at Mahukona (this study) and the rejuvenated stage at Niihau [*Dixon et al.*, 2008]. The inference that recycled ancient carbonate-rich sediments are present in the Hawaiian plume is critical to our understanding of the partial melting of the Hawaiian plume, because even trace amounts of CO_2 generated from carbonate significantly lower the solidus temperature of peridotite. In addition, the presence of CO_2 also significantly modifies the major element compositions of the ensuing melts [e.g., *Dasgupta and Hirschmann*, 2006; *Dasgupta et al.*, 2007].

4.5. Timing of Recycling of Carbonate Sediments

[29] In sections 4.3 and 4.4, we showed that recycled ancient carbonate-rich sediments are present in the Hawaiian plume, which requires that recycling of carbonate-rich sediments into the mantle was occurring early in Earth's history (~2 Ga). Precambrian carbons are common, but we have no constraints on the Sr abundance of the inferred recycled carbonate [e.g., *Veizer et al.*, 1989]. In our model calculation in Figure 12c, we used 2000 ppm Sr in the recycled carbonate component, which implies that this carbonate component is aragonitic, instead of dolomitic, in composition. Aragonate precipitation may have been common in the Precambrian [e.g., *Grotzinger and Reed*, 1983]. If a dolomitic end-member with low Sr abundance (~500 ppm) is used in the model calculation, a larger proportion (up to 6%) of recycled ancient carbonate component is required to explain the observed Rb/Sr and $^{87}Sr/^{86}Sr$ ranges in Mahukona lavas (Figure 12c).

[30] Since Precambrian carbonates are dominated by inorganic $CaCO_3$ precipitates [cf. *Ridgwell and Zeebe*, 2005] and deep-sea carbonates were absent in the Precambrian, it is assumed that organically derived carbonate-rich sediments were not recycled into the mantle through subduction zones until the Paleozoic, when a deep-sea carbonate sink began to form because of carbonate biomineralization (~500 Ma) [*Ridgwell and Zeebe*, 2005, and references therein]. Although stromatolites, which may have an organic origin, are common in Precambrian carbonates [*Grotzinger and Knoll*, 1999, and references therein], they formed in shallow water because photosynthesis was required in their formation in the Precambrian. Consequently, they are not good candidates for recycled carbonates. However, deep-sea carbonates may not be necessary for recycling of carbonates into the mantle. In the Precambrian, carbonate-rich sediments may have been recycled at shallow subduction zones, or by subduction of basaltic oceanic plateaus overlain by shallow water carbonates.

4.6. Size of Geochemical Heterogeneities Within the Hawaiian Plume

[31] The geochemical heterogeneity of a Hawaiian volcano is not proportional to its volume. For example, lavas from Mahukona volcano, with a volume of 13.5×10^3 km^3, have compositional variations similar to those in large Hawaiian volcanoes, such as Mauna Loa (74.0×10^3 km^3) and Mauna Kea (41.9×10^3 km^3) (Figures 2 and 3). Specifically, the variation in $^{143}Nd/^{144}Nd$ of lavas from a given volcano, measured by one standard deviation of $^{143}Nd/^{144}Nd$ within this Hawaiian volcano, does not correlate with its volume, and Koolau volcano is much more heterogeneous than any other Hawaiian volcano (Figure 15). Major and trace element compositions in melt inclusions in olivines from a single lava flow are as variable as those exhibited in whole rocks from different Hawaiian shields [*Ren et al.*, 2005]. Therefore, the size of the geochemical heterogeneities within the Hawaiian plume must be much smaller than the source region of a Hawaiian volcano. Since each

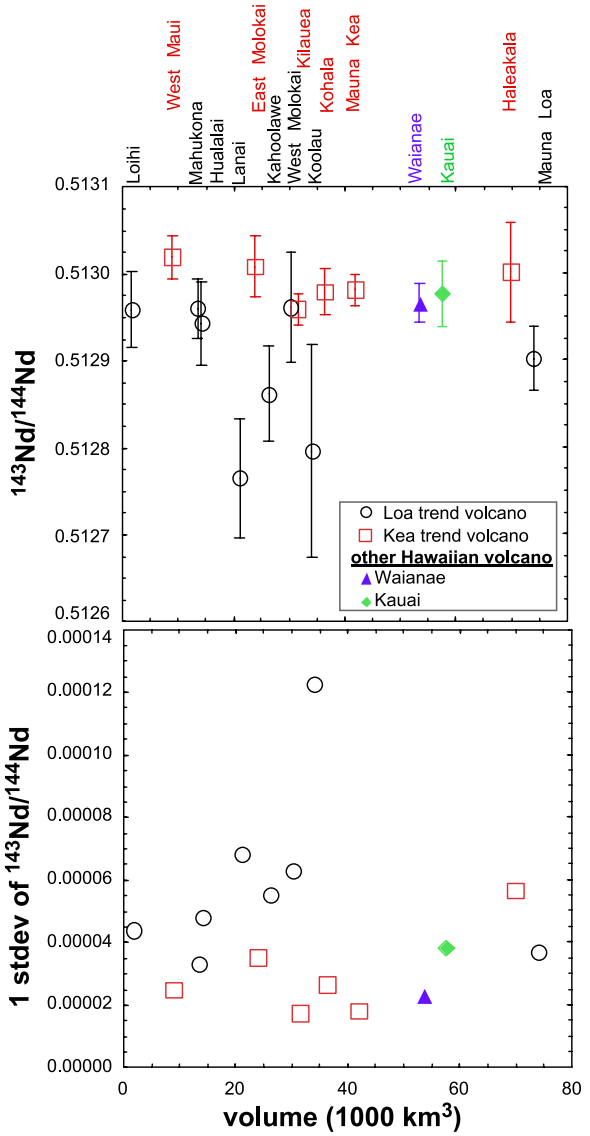

Figure 15. Volume (in 1000 km^3) versus average $^{143}Nd/^{144}Nd$ (with 1 standard deviation bar) and 1 standard deviation of $^{143}Nd/^{144}Nd$ for different Hawaiian tholeiitic shields. Volume data are from *Robinson and Eakins* [2006]. Volcano names are labeled on the top.

Hawaiian volcano is fed from a magma capture zone with a radius ranging from 25 to 34 km [e.g., *DePaolo and Stolper*, 1996; *Ribe and Christensen*, 1999; *DePaolo et al.*, 2001; *Blichert-Toft et al.*, 2003; *Bryce et al.*, 2005], we infer that the upper limit of the size of geochemical heterogeneities within the Hawaiian plume is less than 25–34 km.

[32] Using the $^{176}Hf/^{177}Hf$ and $^{207}Pb/^{204}Pb$ fluctuations in phase 2 of the Hawaii Scientific Drilling Project (HSDP2) drill core, *Blichert-Toft et al.* [2003] argued that the spacing of the geochemical heterogeneities within the mantle source of Mauna Kea volcano is 7–160 km, depending on the radius of the Hawaiian plume conduit. Using Pb isotopic data from the same drill core, *Eisele et al.* [2003] estimated that the minimum length scale of Pb isotopic heterogeneity within the mantle source of Mauna Kea volcano is 21 to 86 km [see *Eisele et al.*, 2003, Figure 13e]. On the basis of the depth profiles of Al_2O_3/CaO, La/Nb, Sr/Nb and Th/La observed in the Koolau Scientific Drilling Project drill core, *Huang and Frey* [2005] argued that the sizes of garnet pyroxenites within the mantle source of Koolau volcano is 2.9 to 29 km.

4.7. Geochemical Structure of the Hawaiian Plume: Concentrically Zoned, Bilaterally Asymmetrical, or Vertically Heterogeneous?

[33] Most lavas erupted along the spatially defined Loa and Kea trends (Figure 1) differ in major and trace element abundances, and Sr-Nd-Hf-Pb isotopic ratios [e.g., *Lassiter et al.*, 1996; *Blichert-Toft et al.*, 2003; *Abouchami et al.*, 2005; *Huang et al.*, 2005b; *Xu et al.*, 2007a]. For example lavas from Mahukona's Loa trend neighbors Kahoolawe and Hualalai (Figure 1), and many Mahukona lavas show distinctive Loa-type geochemical signatures with high $^{208}Pb^*/^{206}Pb^*$ [e.g., *Cousens et al.*, 2003; *Abouchami et al.*, 2005; *Huang et al.*, 2005b; *Xu et al.*, 2005] (Figure 6). Lavas from Kohala, the Kea trend neighbor of Mahukona, have low $^{208}Pb^*/^{206}Pb^*$ and show a distinctive Kea-type signature [e.g., *Abouchami et al.*, 2005] (Figure 6). The geochemical differences between Loa and Kea trend lavas are inferred to reflect source characteristics, and different models of the geochemical structure of the Hawaiian plume have been proposed to explain the geochemical differences between Loa and Kea trend lavas [e.g., *Lassiter et al.*, 1996; *Lassiter and Hauri*, 1998; *DePaolo et al.*, 2001; *Blichert-Toft et al.*, 2003; *Kurz et al.*, 2004; *Abouchami et al.*, 2005; *Bryce et al.*, 2005; *Herzberg*, 2005; *Huang et al.*, 2005b; *Ren et al.*, 2005].

[34] Two types of plume structure have been proposed to explain the geochemical difference between Loa and Kea trend lavas: a concentrically zoned plume model [*Lassiter et al.*, 1996; *DePaolo et al.*, 2001; *Bryce et al.*, 2005] (Figure 16a) based on the fluid dynamical model by *Hauri et al.* [1994] and its modification, a grossly concentrically zoned plume model [*Kurz et al.*, 2004] (Figure 16b) versus a bilaterally asymmetrical plume model [*Abouchami et al.*, 2005] built on the numerical modeling of Farnetani and coworkers

[*Farnetani et al.*, 2002; *Samuel and Farnetani*, 2003] (Figure 16c).

[35] Alternatively, *Blichert-Toft et al.* [2003] and *Blichert-Toft and Albarède* [2009] argued that there are both vertical and radial geochemical heterogeneities in the Hawaiian plume. Using the compositional variability of melt inclusions, *Ren et al.* [2005] presented a variant of this model. The observed geochemical variations in lavas represent the integrated geochemical heterogeneities in both horizontal and vertical directions in the Hawaiian plume [*Blichert-Toft et al.*, 2003, Figure 12]. We note, however, that even though *Eisele et al.* [2003] and *Abouchami et al.* [2005] emphasized vertical homogeneity within the Hawaiian plume, they noted that [*Abouchami et al.*, 2005, p. 851] "both vertical and horizontal variability are likely, but dynamic modeling suggests a dominance of vertical stretching during plume ascent."

[36] It is interesting that two recent papers, *Blichert-Toft and Albarède* [2009] and *Farnetani and Hofmann* [2009], started out with the same analytical formulation of the flow problem [*Olson et al.*, 1993] (*Blichert-Toft and Albarède* [2009, Figure 8] versus *Farnetani and Hofmann* [2009, Figure 1a]), but reached different conclusions (*Blichert-Toft and Albarède* [2009, Figure 9] versus *Farnetani and Hofmann* [2009, Figure 4]). In detail, in the model of *Blichert-Toft and Albarède* [2009], the geochemical heterogeneities are only stretched significantly at the plume edge (the "sheath"), where upwelling velocity and excess potential temperature are low, and much less deformed in the hot plume center [*Blichert-Toft and Albarède*, 2009, Figure 9]. Importantly, the elongation of the heterogeneities in all cases remains much shorter than the length of the plume conduit. Consequently, they suggest that the plume conduit should have [*Blichert-Toft et al.*, 2003, p. 199] "an overall concentric structure ... with a mobile inner core with little stretching," implying vertical heterogeneities within the plume.

[37] In contrast, in the model of *Farnetani and Hofmann* [2009], elongated "spaghettis" are present in both the edge and the center of the plume [*Farnetani and Hofmann*, 2009, Figure 4]. This model differs from that of *Blichert-Toft and*

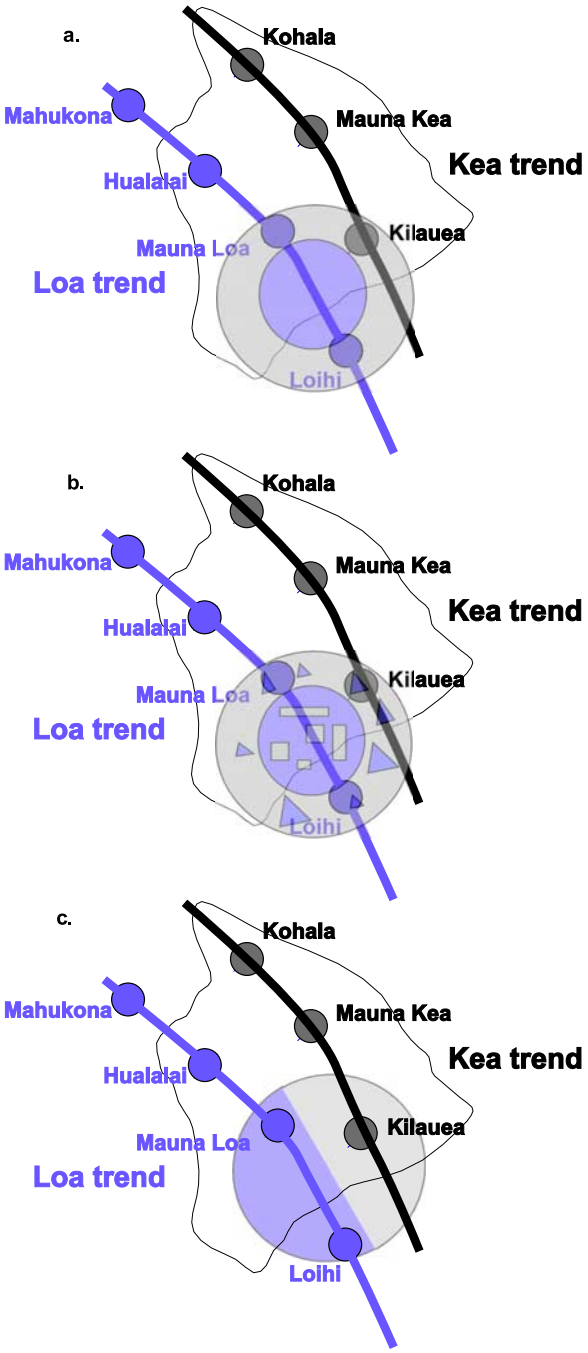

Figure 16. Cartoons showing different models of the geochemical structure of the Hawaiian plume. The blue and gray colors represent different geochemical signatures. (a) A concentrically zoned plume model [e.g., *Lassiter et al.*, 1996; *Bryce et al.*, 2005]. (b) As in Figure 16a but with local Loa-type components in the rim of the plume and local Kea-type components in the core of the plume [*Kurz et al.*, 2004]. The gray rectangles within the blue circle represent Kea-type geochemical heterogeneities in a Loa-type matrix, which dominates the core of the plume, and the blue triangles within the gray ring represent Loa-type geochemical heterogeneities in a Kea-type matrix, which dominates the rim of the plume. (c) A bilaterally asymmetrical zoned plume model [*Abouchami et al.*, 2005].

Albarède [2009] only in that the geochemical heterogeneities are substantially prestretched at the base of the mantle before entering into the plume conduit itself [see *Farnetani and Hofmann*, 2009, right-hand sides of Figures 3 and 4], thus accounting for the observed stretching in the plume center not seen in the model by *Blichert-Toft and Albarède* [2009], in which all heterogeneities start out spherical. In other words, stretching caused by upwelling within the plume conduit itself is essentially identical in both models [see *Farnetani and Hofmann*, 2009, Figure 2; *Blichert-Toft and Albarède*, 2009, Figure 8]. We note that the stretching at the base of the mantle in the model of *Farnetani and Hofmann* [2009] takes place outside of the plume conduit and, hence is not relevant to plume dynamics, but rather is part of the overall dynamical regime of mantle convection. Finally, heterogeneity "trains" are present in the model of *Farnetani and Hofmann* [2009] [see *Farnetani and Hofmann*, 2009, Figure 7] as suggested in the original model of *Blichert-Toft et al.* [2003].

[38] In fact, vertical heterogeneities have been invoked in many published studies. *Bryce et al.* [2005] introduced vertical heterogeneities into a concentrically zoned plume model to explain the observed $^{87}Sr/^{86}Sr$ and $^{143}Nd/^{144}Nd$ variations in several volcanoes on the island of Hawaii [*Bryce et al.*, 2005, Figure 17]. *Marske et al.* [2007] found that recent lavas from Kilauea and Mauna Loa, which usually have distinctive isotopic ratios of Sr, Nd and Pb, converge to similar intermediate ratios during the time interval from AD 250 to 1400; they interpreted this atypical isotopic similarity of Kilauea (Kea trend) and Mauna Loa (Loa trend) as reflecting an isotopically distinct component simultaneously incorporated into the melting regions of both volcanoes. That is, vertical heterogeneity was invoked. On the basis of the observation that the Loa-type geochemical signature is not present in volcanoes/seamounts older than Koolau, *Tanaka et al.* [2008] argued that its presence in young (<3 Ma) Hawaiian volcanoes is episodic. Again, vertical heterogeneity was emphasized.

[39] Although Loa and Kea trend lavas show distinctive geochemical signatures, there are examples of the Loa-type signature in Kea trend volcanoes, and vice versa. *Abouchami et al.* [2005] noted that at Mauna Kea, the HSDP2 "Kea-hi8" lavas, which are equivalent to the HSDP2 low-SiO_2 tholeiitic lavas [*Huang and Frey*, 2003; *Rhodes and Vollinger*, 2004; *Stolper et al.*, 2004], are Loa-like in a $^{206}Pb/^{204}Pb$-$^{208}Pb/^{204}Pb$ plot, and they argued that these HSDP2 low-SiO_2 tholeiitic lavas [*Abouchami et al.*, 2005, p. 852] "represent a local heterogeneity within the plume." That is, vertical heterogeneity is implied [see *Eisele et al.*, 2003, Figure 13]. *Xu et al.* [2007a] observed both Loa-type and Kea-type lavas in West Molokai, the oldest Loa trend volcano on the subparallel portion of the Loa and Kea trends (Figure 1). *Xu et al.* [2007a] adopted the bilaterally asymmetrical plume model [*Abouchami et al.*, 2005] and argued that during the formation of West Molokai, the direction of the relative motion between the Hawaiian plume and the Pacific plate was changing; consequently, the magma capture zone of West Molokai crossed the Kea-Loa boundary within the Hawaiian plume. This interpretation is consistent with the Loa-like geochemical characteristics of Penguin Bank, a submarine volcano west of West Molokai Volcano [*Xu et al.*, 2007a, 2007b].

[40] Our new geochemical data on Mahukona lavas are an example of the Kea-type geochemical signature present in a Loa trend volcano. In detail, Mahukona lavas are within the overlapping region of Loa and Kea trend lavas in a $^{208}Pb^*/^{206}Pb^*$-$^{176}Hf/^{177}Hf$ plot (Figure 7). In a $^{206}Pb/^{204}Pb$-$^{208}Pb/^{204}Pb$ plot, although Mahukona postshield transitional lavas and high-CaO tholeiitic lavas are clearly on the Loa side, Group B tholeiitic lavas straddle the Loa-Kea dividing line and Group A tholeiitic lavas are clearly on the Kea side (Figure 6). Also in a $[CaO]_{10} - [Yb]_{10}$ plot (Figure 9), Mahukona lavas overlap with the Mauna Kea trend, which is perpendicular to the positive $[CaO]_{10} - [Yb]_{10}$ trend defined by Loa lavas. In summary, distinctive Kea-type geochemical (both isotopic and compositional) signatures are shown in lavas from Mahukona, a Loa trend volcano, and are most prominent in Mahukona Group A tholeiitic lavas (Figures 6 and 9). These features cannot be explained by a purely bilateral asymmetrical plume model [*Abouchami et al.*, 2005]. Vertical geochemical heterogeneity can explain the occurrence of Kea-type geochemical signatures in Mahukona volcano.

[41] In summary, in order to explain the observed geochemical variations in modern Hawaiian volcanoes, vertical geochemical heterogeneity has to be called upon in either a concentrically zoned plume model [e.g., *Bryce et al.*, 2005] or a bilaterally asymmetrical plume model [*Marske et al.*, 2007; this study]. Further, we note that if vertical heterogeneity plays an important role [e.g., *Blichert-Toft*

et al., 2003; *Blichert-Toft and Albarède*, 2009], a concentrically zoned plume model and a bilaterally asymmetrical plume model cannot be distinguished from each other using geochemical observations of the volcanoes, because any geochemical observation that is inconsistent with the prediction of a certain type of plume model can be attributed to vertical heterogeneity.

5. Conclusions

[42] 1. Postshield stage transitional lavas and shield stage tholeiitic lavas have been recovered from the submarine Mahukona volcano. Despite being a relatively small volcano, Mahukona tholeiitic lavas show major and trace element abundance variations similar to those observed in large Hawaiian volcanoes.

[43] 2. Mahukona tholeiitic lavas range widely in $[Nb]_{10}$, $[La]_{10}$ and $[Yb]_{10}$, but these differences cannot be explained by variable extents of partial melting of a single spinel or garnet peridotite source. Consequently, we infer that mixing between magmas formed from different source components is important.

[44] 3. On the basis of CaO content, Mahukona tholeiitic lavas can be divided into three groups that form a negative $[CaO]_{10} - [Yb]_{10}$ trend. The CaO difference among different Mahukona CaO groups cannot be explained as a result of sampling different amounts of partial melts derived from garnet pyroxenite (eclogite), characterized by low CaO and Yb contents, or by sampling different amounts of carbonatite, characterized by high CaO and Yb contents. Rather, there is a broad correlation between $[CaO]_{10}$ and $^{143}Nd/^{144}Nd$, implying source heterogeneity. The Mahukona high-CaO lavas have the lowest SiO_2 contents among Mahukona tholeiitic lavas, a feature consistent with partial melting of a carbonate-bearing peridotite; consequently, we infer that the Mahukona high-CaO lavas sampled larger amounts of partial melts of a carbonate-bearing peridotite.

[45] 4. Within Mahukona lavas, $^{87}Sr/^{86}Sr$ is decoupled from Nd, Hf and Pb isotopic ratios, but is correlated with trace element abundance ratios involving Sr. These correlations, especially the negative Rb/Sr-$^{87}Sr/^{86}Sr$ trend, are best explained as mixing lines. Furthermore, we note that different Hawaiian shields also define a negative Rb/Sr-$^{87}Sr/^{86}Sr$ correlation. We infer that a recycled ancient carbonate-rich sedimentary component contributed to Hawaiian lavas. In conjunction with the arguments from *Huang and Frey* [2005] and *Dixon et al.* [2008], we deduce that carbonates are ubiquitous in the Hawaiian plume. This inference has important implications for the partial melting of the Hawaiian plume, since CO_2 substantially lowers the solidus temperature of mantle peridotite, and for the volatile budget of Hawaiian lavas. In addition, the requirement of recycled ancient carbonate-rich sediments in the Hawaiian plume implies that carbonate-rich sediments were returned to the mantle through subduction zones in the Precambrian, which has important implications for the global carbon cycle.

[46] 5. Mahukona Group A tholeiitic lavas show distinctive Kea-type isotopic and trace element signatures, a feature inconsistent with a bilaterally asymmetrical plume model. Consequently, vertical heterogeneity within the plume is required.

Appendix A: Analytical Methods

[47] Major and some trace element abundances of most samples were analyzed by XRF at University of Massachusetts following methods modified from *Norrish and Chappell* [1967] and *Norrish and Hutton* [1969], while the D6 samples were analyzed by XRF at Washington State University (Tables 1 and 2). Other trace element abundances (Table 3) were determined by ICP-MS at the GeoAnalytical Laboratory of Washington State University following the method of *Knaack et al.* [1994].

[48] Strontium and Nd isotopic ratios (Table 4a) were determined on acid-leached samples at Florida State University (FSU) following the leaching procedure described by *Huang et al.* [2005a]. In detail, ~0.2–0.4 g whole rock powders or chips were step-leached using 6N HCl until the acid was colorless or pale yellow. The leached residues were then dissolved using mixed HF-HNO_3. Strontium and rare earth elements (REEs) were separated from the matrix using cation exchange resin, and Nd was further separated from the other REEs using HDEHP columns. $^{87}Sr/^{86}Sr$ was measured on the Finnigan® MAT 262 TIMS located within the Geochemistry Group in the National High Magnetic Field Laboratory of FSU. The E&A Sr standard gave an average of 0.708002 ± 0.000011 (2 S.D., n = 8) for $^{87}Sr/^{86}Sr$ during the course of this study.

[49] Neodymium isotopic ratios (Table 4a) were determined on the ThermoFinnigan Neptune® MC-ICP-MS with an ESI Apex® nebulizer at FSU, and mass fractionation was corrected relative to

$^{146}Nd/^{144}Nd$ = 0.7219. The LaJolla Nd standard was analyzed every 4–5 samples in order to monitor instrument performance. Ratios of $^{143}Nd/^{144}Nd$ are reported relative to $(^{143}Nd/^{144}Nd)_{LaJolla}$ = 0.511850. Samples D6-R3 and D6-R6 were also analyzed for $^{87}Sr/^{86}Sr$ and $^{143}Nd/^{144}Nd$ (Table 4a) on a Triton® TIMS at Carleton University following the method described by *Cousens* [1996]. The data from the two labs (FSU and Carleton) are in good agreement.

[50] Hafnium isotopic ratios (Table 4a) were determined on unleached samples at the Ecole Normale Supérieure in Lyon (ENSL) following the procedure described by *Blichert-Toft et al.* [1997] using a Nu Plasma® MC-ICP-MS coupled with a desolvating nebulizer DSN-100. Instrumental mass bias was corrected relative to $^{179}Hf/^{177}Hf$ = 0.7325 using an exponential law. The Hf standard JMC-475 was analyzed systematically in between every two to four samples and gave an average $^{176}Hf/^{177}Hf = 0.282160 \pm 0.000010$ (2σ). The total procedural Hf blank was better than 20 pg. Four samples also were analyzed for $^{176}Hf/^{177}Hf$ on acid-leached residues at FSU. For these samples, Hf was separated from the matrix using the separation method described by *Münker et al.* [2001]. The Hf isotopic ratios were measured on the ThermoFinnigan Neptune® MC-ICP-MS with an ESI Apex® nebulizer, and mass fractionation was corrected relative to $^{179}Hf/^{177}Hf$ = 0.7325. The Hf standard JMC-475 was analyzed every four samples to monitor instrument performance. $^{176}Hf/^{177}Hf$ are reported relative to $(^{176}Hf/^{177}Hf)_{JMC\text{-}475}$ = 0.282160. The $^{176}Hf/^{177}Hf$ data from the two labs (ENSL and FSU) are within the analytical 2σ (Table 4a).

[51] Lead isotopic ratios in 17 Mahukona samples (Table 4b) were determined on acid-leached residues at the Max-Planck-Institut für Chemie (Mainz) using the triple-spike technique as described by *Abouchami et al.* [2000]. Rock chips (0.1–0.2 g) were used for Pb isotopic analysis. To remove contaminants, the chips were first rinsed with deionized water, leached with hot 6N HCl for 1 h, and repeatedly rinsed with deionized water until the water was colorless prior to dissolution. Following dissolution, Pb was separated using the mixed HBr-HNO_3 anion exchange technique. The Pb isotopic ratios were determined on a ThermoElectron Triton® TIMS operating in static multicollector mode and corrected for instrumental mass bias using the triple spike technique [*Galer*, 1999]. The NIST SRM-981 standard was analyzed systematically during the course of data collection and gave, on average, $^{206}Pb/^{204}Pb = 16.9432 \pm 0.0015$, $^{207}Pb/^{204}Pb = 15.5015 \pm 0.0016$ and $^{208}Pb/^{204}Pb = 36.7313 \pm 0.0041$ (2 S.D., n = 26). The procedural Pb blank analyzed in parallel with the samples was 19 pg.

[52] Lead isotopic ratios in six Mahukona samples were also determined on acid-leached residues at FSU, including two duplicate analyses (F288HW-D18-6 and P5-72-1). Pb was separated from the matrix using anion exchange resin and HBr. The Pb isotopic ratios were determined on the ThermoFinnigan Neptune® MC-ICP-MS with an ESI Apex® nebulizer using the Tl-doping technique [*White et al.*, 2000]. Mass fractionation was corrected using $^{203}Tl/^{205}Tl$ = 0.418922. The NIST SRM-981 standard was analyzed every 4–5 samples in order to monitor instrument performance. The Pb isotopic ratios in these six samples are reported relative to the average Pb isotopic ratios of the NIST SRM-981 standard obtained from the Max-Planck-Institut (Table 4b). The duplicate Pb analyses between the two labs (Mainz and FSU) exceed the analytical 2σ, but are within 0.2‰ per amu. This discrepancy does not affect subsequent interpretations.

Acknowledgments

[53] This research was supported by NSF grant EAR-0607895 to FAF. D.A.C. was supported through a grant to the Monterey Bay Aquarium Research Institute from the David and Lucile Packard Foundation. J.B.T. acknowledges financial support from the French Institut National des Sciences de l'Univers. Initial isotopic work by B.L.C. was supported by MBARI under a contract. The MC-ICP-MS in the Plasma Analytical Facility at FSU was partially funded by NSF grant EAR 0521201 (to V. J. M. Salters). The *Pisces V* submersible samples were collected under a grant from the Hawaii Undersea Research Laboratory to James Moore and D.A.C. The D6 transitional samples were recovered during cruise TUIM01 funded by NSF grant OCE-00-02470 to Gabi Laske. The other dredge samples were collected during U.S. Geological Survey cruise F2-88-HW, D.A.C. chief scientist. S.H. thanks M. Bizimis, N. J. Tibbetts, S. Mallick, and T. Zateslo for help with the chemical analyses. M. Bizimis, V. J. M. Salters, J. Farkaš, S. W. Wise, A. L. Odom, S. A. Kish, G. Dix, and J. Chiarenzelli are thanked for discussions. We thank R. Dasgupta and an anonymous reviewer for their constructive and helpful comments and V. J. M. Salters for his editorial handling as well as his insightful comments.

References

Abouchami, W., S. J. G. Galer, and A. W. Hofmann (2000), High precision lead isotope systematics of lavas from the

Hawaiian Scientific Drilling Project, *Chem. Geol.*, *169*, 187–209, doi:10.1016/S0009-2541(00)00328-4.

Abouchami, W., A. W. Hofmann, S. J. G. Galer, F. A. Frey, J. Eisele, and M. Feigenson (2005), Lead isotopes reveal bilateral asymmetry and vertical continuity in the Hawaiian mantle plume, *Nature*, *434*, 851–856, doi:10.1038/nature03402.

Balta, J. B., P. D. Asimow, and J. L. Mosenfelder (2008), Carbon-free melting of fertile garnet peridotite in water-undersaturated systems*Eos Trans. AGU*, *89*(53), Fall Meet. Suppl., Abstract V43B-2149.

Bizimis, M., V. J. M. Salters, and J. B. Dawson (2003), The brevity of carbonatite sources in the mantle: Evidence from Hf isotopes, *Contrib. Mineral. Petrol.*, *145*, 281–300, doi:10.1007/s00410-003-0452-3.

Blichert-Toft, J., and F. Albarède (1997), The Lu-Hf isotope geochemistry of chondrites and the evolution of the mantle-crust system, *Earth Planet. Sci. Lett.*, *148*, 243–258, doi:10.1016/S0012-821X(97)00040-X.

Blichert-Toft, J., and F. Albarède (2009), Mixing of isotopic heterogeneities in the Mauna Kea plume conduit, *Earth Planet. Sci. Lett.*, *282*, 190–200, doi:10.1016/j.epsl.2009.03.015.

Blichert-Toft, J., C. Chauvel, and F. Albarède (1997), Separation of Hf and Lu for high-precision isotope analysis of rock samples by magnetic sector-multiple collector ICP-MS, *Contrib. Mineral. Petrol.*, *127*, 248–260, doi:10.1007/s004100050278.

Blichert-Toft, J., F. A. Frey, and F. Albarede (1999), Hf isotope evidence for pelagic sediments in the source of Hawaiian basalts, *Science*, *285*(5429), 879–882, doi:10.1126/science.285.5429.879.

Blichert-Toft, J., D. Weis, C. Maerschalk, A. Agranier, and F. Albarède (2003), Hawaiian hot spot dynamics as inferred from the Hf and Pb isotope evolution of Mauna Kea volcano, *Geochem. Geophys. Geosyst.*, *4*(2), 8704, doi:10.1029/2002GC000340.

Bryce, J. G., D. J. DePaolo, and J. C. Lassiter (2005), Geochemical structure of the Hawaiian plume: Sr, Nd, and Os isotopes in the 2.8 km HSDP-2 section of Mauna Kea volcano, *Geochem. Geophys. Geosyst.*, *6*, Q09G18, doi:10.1029/2004GC000809.

Castillo, P. R., E. Klein, J. Bender, C. Langmuir, S. Shirey, R. Batiza, and W. White (2000), Petrology and Sr, Nd, and Pb isotope geochemistry of mid-ocean ridge basalt glasses from the 11°45′N to 15°00′N segment of the East Pacific Rise, *Geochem. Geophys. Geosyst.*, *1*(11), 1011, doi:10.1029/1999GC000024.

Chen, C.-Y., and F. A. Frey (1985), Trace element and isotope geochemistry of lavas from Haleakala Volcano, East Maui: Implications for the origin of Hawaiian basalts, *J. Geophys. Res.*, *90*(B10), 8743–8768, doi:10.1029/JB090iB10p08743.

Clague, D. A., and A. T. Calvert (2009), Postshield Stage Transitional Volcanism on Mahukona volcano, Hawaii, *Bull. Volcanol.*, doi:10.1007/s00445-008-0240-z, in press.

Clague, D. A., and G. B. Dalrymple (1987), The Hawaiian-Emperor volcanic chain, part 1, *U.S. Geol. Surv. Prof. Pap.*, *1350*, 5–54.

Clague, D. A., and F. A. Frey (1982), Petrology and trace element geochemistry of the Honolulu volcanics, Oahu: Implications for the oceanic mantle below Hawaii, *J. Petrol.*, *23*, 447–504.

Clague, D. A., and J. G. Moore (1991a), Geology and petrology of Mahukona volcano, Hawaii, *Bull. Volcanol.*, *53*, 159–172, doi:10.1007/BF00301227.

Clague, D. A., and J. G. Moore (1991b), Comment on "Mahukona: The missing Hawaiian volcano", by M. O. Garcia, M. D. Kurz, and D. W. Muenow, *Geology*, *19*, 1049–1050, doi:10.1130/0091-7613(1991)019<1049:CAROMT>2.3.CO;2.

Cohen, A. S., R. K. O'Nions, and M. D. Kurz (1996), Chemical and isotopic variations in Mauna Loa tholeiites, *Earth Planet. Sci. Lett.*, *143*, 111–124, doi:10.1016/0012-821X(96)00131-8.

Cousens, B. L. (1996), Magmatic evolution of Quaternary mafic magmas at Long Valley Caldera and the Devils Postpile, California: Effects of crustal contamination on lithospheric mantle-derived magmas, *J. Geophys. Res.*, *101*, 27,673–27,689, doi:10.1029/96JB02093.

Cousens, B. L., D. A. Clague, and W. D. Sharp (2003), Chronology, chemistry, and origin of trachytes from Hualalai Volcano, Hawaii, *Geochem. Geophys. Geosyst.*, *4*(9), 1078, doi:10.1029/2003GC000560.

Dasgupta, R., and M. M. Hirschmann (2006), Melting in the Earth's deep upper mantle caused by carbon dioxide, *Nature*, *440*, 659–662, doi:10.1038/nature04612.

Dasgupta, R., M. M. Hirschmann, and N. D. Smith (2007), Partial melting experiments of peridotite + CO_2 at 3 GPa and genesis of alkalic ocean island basalts, *J. Petrol.*, *48*, 2093–2124, doi:10.1093/petrology/egm053.

Dasgupta, R., M. M. Hirschmann, W. F. McDonough, M. Spiegelman, and A. C. Withers (2009), Trace element partitioning between garnet lherzolite and carbonatite at 6.6 and 8.6 GPa with applications to the geochemistry of the mantle and of mantle-derived melts, *Chem. Geol.*, *262*, 57–77, doi:10.1016/j.chemgeo.2009.02.004.

Davis, F. A., M. Wick, A. C. Withers, and M. M. Hirschmann (2008), Determining low-degree partial melts of garnet peridotite at 3 GPa by Modified Iterative Sandwich Experiments (MISE), *Eos Trans. AGU*, *89*(53), Fall Meet. Suppl., Abstract V41D-2133.

DePaolo, D. J., and E. M. Stolper (1996), Models of Hawaiian volcano growth and plume structure: Implications of results from the Hawaii Scientific Drilling Project, *J. Geophys. Res.*, *101*, 11,643–11,654, doi:10.1029/96JB00070.

DePaolo, D. J., J. G. Bryce, A. Dodson, D. L. Shuster, and B. M. Kennedy (2001), Isotopic evolution of Mauna Loa and the chemical structure of the Hawaiian plume, *Geochem. Geophys. Geosyst.*, *2*(7), 1044, doi:10.1029/2000GC000139.

Dixon, J., D. A. Clague, B. Cousens, M. L. Monsalve, and J. Uhl (2008), Carbonatite and silicate melt metasomatism of the mantle surrounding the Hawaiian plume: Evidence from volatiles, trace elements, and radiogenic isotopes in rejuvenated-stage lavas from Niihau, Hawaii, *Geochem. Geophys. Geosyst.*, *9*, Q09005, doi:10.1029/2008GC002076.

Eggins, S. M., R. L. Rudnick, and W. F. McDonough (1998), The composition of peridotites and their minerals: A laser ablation ICP-MS study, *Earth Planet. Sci. Lett.*, *154*, 53–71, doi:10.1016/S0012-821X(97)00195-7.

Eiler, J. M., K. A. Farley, J. W. Valley, A. W. Hofmann, and E. M. Stolper (1996), Oxygen isotope constraints on the sources of Hawaiian volcanism, *Earth Planet. Sci. Lett.*, *144*, 453–468, doi:10.1016/S0012-821X(96)00170-7.

Eisele, J., W. Abouchami, S. J. G. Galer, and A. W. Hofmann (2003), The 320 kyr Pb isotope evolution of Mauna Kea lavas recorded in the HSDP-2 drill core, *Geochem. Geophys. Geosyst.*, *4*(5), 8710, doi:10.1029/2002GC000339.

Farnetani, C. G., and A. W. Hofmann (2009), Dynamics and internal structure of a lower mantle plume conduit, *Earth*

Planet. Sci. Lett., *282*, 314–322, doi:10.1016/j.epsl.2009.03.035.

Farnetani, C. G., B. Legras, and P. J. Tackley (2002), Mixing and deformations in mantle plumes, *Earth Planet. Sci. Lett.*, *196*, 1–15, doi:10.1016/S0012-821X(01)00597-0.

Fekiacova, Z., W. Abouchami, S. J. G. Galer, M. O. Garcia, and A. W. Hofmann (2007), Origin and temporal evolution of Ko'olau volcano, Hawai'i: Inferences from isotope data on the Ko'olau Scientific Drilling Project (KSDP), the Honolulu Volcanics and ODP Site 843, *Earth Planet. Sci. Lett.*, *261*, 65–83, doi:10.1016/j.epsl.2007.06.005.

Frey, F. A. (1980), The origin of pyroxenites and garnet pyroxenites from Salt Lake Crater, Oahu, Hawaii: Trace element evidence, *Am. J. Sci.*, *280-A*, 427–449.

Frey, F. A., and D. H. Green (1974), The mineralogy, geochemistry and origin of lherzolite inclusions in Victorian basanites, *Geochim. Cosmochim. Acta*, *38*, 1023–1059, doi:10.1016/0016-7037(74)90003-9.

Frey, F. A., and J. M. Rhodes (1993), Inter-shield geochemical differences among Hawaiian volcanoes: Implications for source compositions, melting processes and magma ascent paths, *Philos. Trans. R. Soc. London, Ser. A*, *342*, 121–136, doi:10.1098/rsta.1993.0009.

Frey, F. A., M. O. Garcia, W. S. Wise, A. Kennedy, P. Gurriet, and F. Albarède (1991), The evolution of Mauna Kea volcano, Hawaii: Petrogenesis of tholeiitic and alkalic basalts, *J. Geophys. Res.*, *96*, 14,347–14,375, doi:10.1029/91JB00940.

Frey, F. A., M. O. Garcia, and M. F. Roden (1994), Geochemical characteristics of Koolau Volcano: Implications of intershield geochemical differences among Hawaiian volcanoes, *Geochim. Cosmochim. Acta*, *58*, 1441–1462, doi:10.1016/0016-7037(94)90548-7.

Frey, F. A., D. A. Clague, J. J. Mahoney, and J. M. Sinton (2000), Volcanism at the edge of the Hawaiian plume: Petrogenesis of submarine alkalic lavas from the North Arch volcanic field, *J. Petrol.*, *41*(5), 667–691, doi:10.1093/petrology/41.5.667.

Frey, F. A., S. Huang, J. Blichert-Toft, M. Regelous, and M. Boyet (2005), Origin of depleted components in basalt related to the Hawaiian hot spot: Evidence from isotopic and incompatible element ratios, *Geochem. Geophys. Geosyst.*, *6*, Q02L07, doi:10.1029/2004GC000757.

Gaffney, A. M., B. K. Nelson, and J. Blichert-Toft (2004), Geochemical constraints on the role of oceanic lithosphere in intra-volcano heterogeneity at West Maui, Hawaii, *J. Petrol.*, *45*, 1663–1687, doi:10.1093/petrology/egh029.

Galer, S. J. G. (1999), Optimal double and triple spiking for high precision lead isotopic measurement, *Chem. Geol.*, *157*, 255–274, doi:10.1016/S0009-2541(98)00203-4.

Galer, S. J. G., and R. K. O'Nions (1985), Residence time of thorium, uranium and lead in the mantle with implications for mantle convection, *Nature*, *316*, 778–782, doi:10.1038/316778a0.

Garcia, M. O., and M. D. Kurz (1991), Reply to comment on "Mahukona: The missing Hawaiian volcano" by D. A. Clague and J. G. Moore, *Geology*, *19*, 1050–1051.

Garcia, M. O., M. D. Kurz, and D. W. Muenow (1990), Mahukona: The missing Hawaiian volcano, *Geology*, *18*, 1111–1114, doi:10.1130/0091-7613(1990)018<1111:MTMHV>2.3.CO;2.

Garcia, M. O., B. A. Jorgenson, J. J. Mahoney, E. Ito, and A. J. Irving (1993), An evaluation of temporal geochemical evolution of Loihii summit lavas: Results from Alvin submersible dives, *J. Geophys. Res.*, *98*, 535–550.

Garcia, M. O., T. P. Hulsebosch, and J. M. Rhodes (1995a), Olivine-rich submarine basalts from the southwest rift zone of Mauna Loa Volcano: Implications for magmatic processes and geochemical evolution, in *Mauna Loa Revealed: Structure, Composition, History, and Hazards*, *Geophys. Monogr. Ser.*, vol. 92, edited by J. M. Rhodes and J. P. Lockwood, pp. 219–239, AGU, Washington, D. C.

Garcia, M. O., D. J. P. Foss, H. B. West, and J. J. Mahoney (1995b), Geochemical and isotopic evolution of Loihi Volcano, Hawaii, *J. Petrol.*, *36*, 1647–1674.

Garcia, M. O., K. H. Rubin, M. D. Norman, J. M. Rhodes, D. W. Graham, D. W. Muenow, and K. Spencer (1998), Petrology and geochronology of basalt breccia from the 1996 earthquake swarm of Loihi Seamount, Hawaii: Magmatic history of its 1996 eruption, *Bull. Volcanol.*, *59*, 577–592, doi:10.1007/s004450050211.

Garcia, M. O., A. J. Pietruszka, J. M. Rhodes, and K. Swanson (2000), Magmatic processes during the prolonged Pu'u O'o eruption of Kilauea volcano, Hawaii, *J. Petrol.*, *41*(7), 967–990, doi:10.1093/petrology/41.7.967.

Garcia, M. O., E. Ito, and J. M. Eiler (2008), Oxygen isotope evidence for chemical interaction of Kilauea historical magmas with basement rocks, *J. Petrol.*, *49*, 757–769, doi:10.1093/petrology/egm034.

Grotzinger, J. P., and A. H. Knoll (1999), Stromatolites in Precambrian carbonates: Evolutionary mileposts or environmental dipsticks?, *Annu. Rev. Earth Planet. Sci.*, *27*, 313–358, doi:10.1146/annurev.earth.27.1.313.

Grotzinger, J. P., and J. F. Reed (1983), Evidence for primary aragonite precipitation, lower Proterozoic (1.9 Ga) dolomite, Wopmay orogen, northwest Canada, *Geology*, *11*, 710–713, doi:10.1130/0091-7613(1983)11<710:EFPAPL>2.0.CO;2.

Hanson, G. N. (1989), An approach to trace element modeling using a simple igneous system as an example in geochemistry and mineralogy of rare earth elements, *Rev. Mineral.*, *21*, 79–97.

Haskins, E. R., and M. O. Garcia (2004), Scientific drilling reveals geochemical heterogeneity within the Ko'olau shield, Hawai'i, *Contrib. Mineral. Petrol.*, *147*, 162–188.

Hauri, E. H. (1996), Major-element variability in the Hawaiian mantle plume, *Nature*, *382*, 415–419, doi:10.1038/382415a0.

Hauri, E. H., J. A. Whitehead, and S. R. Hart (1994), Fluid dynamic and geochemical aspects of entrainment in mantle plumes, *J. Geophys. Res.*, *99*, 24,275–24,300, doi:10.1029/94JB01257.

Herzberg, C. (2005), Big lessons from little droplets, *Nature*, *436*, 789–790, doi:10.1038/436789b.

Herzberg, C. (2006), Petrology and thermal structure of the Hawaiian plume from Mauna Kea volcano, *Nature*, *444*, 605–609, doi:10.1038/nature05254.

Herzberg, C., and P. D. Asimow (2008), Petrology of some oceanic island basalts: PRIMELT2.XLS software for primary magma calculation, *Geochem. Geophys. Geosyst.*, *9*, Q09001, doi:10.1029/2008GC002057.

Hirschmann, M. M., T. Kogiso, M. B. Baker, and E. M. Stolper (2003), Alkalic magmas generated by partial melting of garnet pyroxenite, *Geology*, *31*, 481–484, doi:10.1130/0091-7613(2003)031<0481:AMGBPM>2.0.CO;2.

Hoernle, K., G. Tilton, M. J. Le Bas, S. Duggen, and D. G. Schönberg (2002), Geochemistry of oceanic carbonatites compared with continental carbonatites: Mantle recycling of oceanic crustal carbonate, *Contrib. Mineral. Petrol.*, *142*, 520–542.

Hofmann, A. W. (1988), Chemical differentiation of the earth: The relationship between mantle, continental crust, and ocea-

nic crust, *Earth Planet. Sci. Lett.*, *90*, 297–314, doi:10.1016/0012-821X(88)90132-X.

Hofmann, A. W., and K. P. Jochum (1996), Source characteristics derived from very incompatible elements in Mauna Loa and Mauna Kea basalts (Hawaiian Scientific Drilling Project), *J. Geophys. Res.*, *101*, 11,831–11,839, doi:10.1029/95JB03701.

Hofmann, A. W., and W. M. White (1982), Mantle plumes from ancient oceanic crust, *Earth Planet. Sci. Lett.*, *57*, 421–436, doi:10.1016/0012-821X(82)90161-3.

Hofmann, A. W., M. D. Feigenson, and I. Raczek (1987), Kohala revisited, *Contrib. Mineral. Petrol.*, *95*, 114–122, doi:10.1007/BF00518034.

Huang, S., and F. A. Frey (2003), Trace element abundances of Mauna Kea basalt from phase 2 of the Hawaii Scientific Drilling Project: Petrogenetic implications of correlations with major element content and isotopic ratios, *Geochem. Geophys. Geosyst.*, *4*(6), 8711, doi:10.1029/2002GC000322.

Huang, S., and F. A. Frey (2005), Recycled oceanic crust in the Hawaiian Plume: Evidence from temporal geochemical variations within the Koolau shield, *Contrib. Mineral. Petrol.*, *149*, 556–575, doi:10.1007/s00410-005-0664-9.

Huang, S., M. Regelous, T. Thordarson, and F. A. Frey (2005a), Petrogenesis of lavas from Detroit Seamount: Geochemical differences between Emperor Chain and Hawaiian volcanoes, *Geochem. Geophys. Geosyst.*, *6*, Q01L06, doi:10.1029/2004GC000756.

Huang, S., F. A. Frey, J. Blichert-Toft, R. V. Fodor, G. R. Bauer, and G. Xu (2005b), Enriched components in the Hawaiian plume: Evidence from Kahoolawe Volcano, Hawaii, *Geochem. Geophys. Geosyst.*, *6*, Q11006, doi:10.1029/2005GC001012.

Huang, S., M. Humayun, and F. A. Frey (2007), Iron/manganese ratio and manganese content in shield lavas from Ko'olau Volcano, Hawai'i, *Geochim. Cosmochim. Acta*, *71*, 4557–4569, doi:10.1016/j.gca.2007.07.013.

Humayun, M., L. Qin, and M. D. Norman (2004), Geochemical evidence for excess iron in the mantle beneath Hawai'i, *Science*, *306*, 91–94.

Jackson, M. G., and R. Dasgupta (2008), Compositions of HIMU, EM1, and EM2 from global trends between radiogenic isotopes and major elements in ocean island basalts, *Earth Planet. Sci. Lett.*, *276*, 175–186, doi:10.1016/j.epsl.2008.09.023.

Jackson, M. G., S. R. Hart, A. A. P. Koppers, H. Staudigel, J. Konter, J. Blusztajn, M. Kurz, and J. A. Russell (2007), The return of subducted continental crust in Samoan lavas, *Nature*, *448*, 684–687, doi:10.1038/nature06048.

Keller, R. A., M. R. Fish, and W. M. White (2000), Isotopic evidence for Late Cretaceous plume-ridge interaction at the Hawaiian hotspot, *Nature*, *405*, 673–676, doi:10.1038/35015057.

Keshav, S., G. H. Gudfinnsson, G. Sen, and Y.-W. Fei (2004), High-pressure melting experiments on garnet clinopyroxenite and the alkalic to tholeiitic transition in ocean-island basalts, *Earth Planet. Sci. Lett.*, *223*, 365–379, doi:10.1016/j.epsl.2004.04.029.

Keshav, S., G. Sen, and D. C. Presnall (2007), Garnet-bearing xenoliths from Salt Lake Crater, Oahu, Hawaii: High-pressure fractional crystallization in the oceanic mantle, *J. Petrol.*, *48*, 1681–1724, doi:10.1093/petrology/egm035.

Knaack, C., S. B. Cornelius, and P. R. Hooper (1994), Trace element analyses of rocks and minerals by ICP-MS, technical note, GeoAnal. Lab, Wash. State Univ., Pullman. (Available at http://www.wsu.edu/~geolab/note/icpms.html)

Kogiso, T., M. M. Hirschmann, and D. J. Frost (2003), High-pressure partial melting of garnet pyroxenite: Possible mafic lithologies in the source of ocean island basalts, *Earth Planet. Sci. Lett.*, *216*, 603–617, doi:10.1016/S0012-821X(03)00538-7.

Kurz, M. D., T. C. Kenna, D. P. Kammer, J. M. Rhodes, and M. O. Garcia (1995), Isotopic evolution of Mauna Loa volcano: A view from the submarine southwest rift, in *Mauna Loa Revealed: Structure, Composition, History, and Hazards*, *Geophys. Monogr. Ser.*, vol. 92, edited by J. M. Rhodes and J. P. Lockwood, pp. 289–306, AGU, Washington, D. C.

Kurz, M. D., J. Curtice, D. E. Lott III, and A. Solow (2004), Rapid helium isotopic variability in Mauna Kea shield lavas from the Hawaiian Scientific Drilling Project, *Geochem. Geophys. Geosyst.*, *5*, Q04G14, doi:10.1029/2002GC000439.

Langmuir, C. H., E. M. Klein, and T. Plank (1992), Petrological systematics of mid-ocean ridge basalts: Constraints on melt generation beneath ocean ridges, in *Mantle Flow and Melt Generation at Mid-Ocean Ridges*, *Geophys. Monogr. Ser.*, vol. 71, edited by J. Phipps Morgan, D. K. Blackman, and J. M. Sinton, pp. 183–280, AGU, Washington, D. C.

Lassiter, J. C., and E. H. Hauri (1998), Osmium-isotope variations in Hawaiian lavas: Evidence for recycled oceanic lithosphere in the Hawaiian plume, *Earth Planet. Sci. Lett.*, *164*, 483–496, doi:10.1016/S0012-821X(98)00240-4.

Lassiter, J. C., D. J. DePaolo, and M. Tatsumoto (1996), Isotopic evolution of Mauna Kea volcano: Results from the initial phase of the Hawaiian Scientific Drilling Project, *J. Geophys. Res.*, *101*, 11,769–11,780, doi:10.1029/96JB00181.

Lassiter, J. C., E. H. Hauri, P. W. Reiners, and M. O. Garcia (2000), Generation of Hawaiian post-erosional lavas by melting of a mixed lherzolite/pyroxenite source, *Earth Planet. Sci. Lett.*, *178*(3–4), 269–284, doi:10.1016/S0012-821X(00)00084-4.

Le Roex, A. P., and R. Lanyon (1998), Isotope and trace element geochemistry of Cretaceous Damaraland lamprophyres and carbonatites, northwestern Namibia: Evidence for plume-lithosphere interactions, *J. Petrol.*, *39*, 1117–1146, doi:10.1093/petrology/39.6.1117.

Longhi, J. (2002), Some phase equilibrium systematics of lherzolite melting: I, *Geochem. Geophys. Geosyst.*, *3*(3), 1020, doi:10.1029/2001GC000204.

Marske, J. P., A. J. Pietruszka, D. Weis, M. O. Garcia, and J. M. Rhodes (2007), Rapid passage of a small-scale mantle heterogeneity through the melting regions of Kilauea and Mauna Loa volcanoes, *Earth Planet. Sci. Lett.*, *259*, 34–50, doi:10.1016/j.epsl.2007.04.026.

McDonough, W. F., and S. Sun (1995), The composition of the Earth, *Chem. Geol.*, *120*, 223–253, doi:10.1016/0009-2541(94)00140-4.

McDougall, I., and D. A. Swanson (1972), Potassium-argon ages of lavas from the Hawi, and Pololu Volcanic Series, Kohala Volcano, Hawaii, *Geol. Soc. Am. Bull.*, *83*, 3731–3738, doi:10.1130/0016-7606(1972)83[3731:PAOLFT]2.0.CO;2.

McKenzie, D., and R. K. O'Nions (1983), Mantle reservoirs and oceanic island basalts, *Nature*, *301*, 229–231, doi:10.1038/301229a0.

Moore, J. G., and D. A. Clague (1992), Volcano growth and evolution of the island of Hawaii, *Geol. Soc. Am. Bull.*, *104*, 1471–1484, doi:10.1130/0016-7606(1992)104<1471:VGAEOT>2.3.CO;2.

Mukhopadhyay, S., J. L. Lassiter, K. A. Farley, and S. W. Bogue (2003), Geochemistry of Kauai shield-stage lavas: Implications for the chemical evolution of the Hawaiian plume, *Geochem. Geophys. Geosyst.*, *4*(1), 1009, doi:10.1029/2002GC000342.

Münker, C., S. Weyer, E. Scherer, and K. Mezger (2001), Separation of high field strength elements (Nb, Ta, Zr, Hf) and Lu from rock samples for MC-ICPMS measurements, *Geochem. Geophys. Geosyst.*, *2*(12), 1064, doi:10.1029/2001GC000183.

Nelson, D. R., A. R. Chivas, B. W. Chappell, and M. T. McCulloch (1988), Geochemical and isotopic systematics in carbonatites and implications for the evolution of ocean-island sources, *Geochim. Cosmochim. Acta*, *52*, 1–17, doi:10.1016/0016-7037(88)90051-8.

Niu, Y., K. D. Collerson, R. Batiza, J. I. Wendt, and M. Regelous (1999), Origin of enriched-type mid-ocean ridge basalt at ridges far from mantle plumes; the East Pacific Rise at 11 degrees 20′N, *J. Geophys. Res.*, *104*(B4), 7067–7087, doi:10.1029/1998JB900037.

Norrish, K., and B. W. Chappell (1967), X-ray fluorescent spectrography, in *Physical Methods in Determinitive Mineralogy*, vol. 24, pp. 65–105, Mineral. Soc. of Am., Washington D. C.

Norrish, K., and J. T. Hutton (1969), An accurate X-ray spectrographic method for the analysis of a wide range of geological samples, *Geochim. Cosmochim. Acta*, *33*, 431–454, doi:10.1016/0016-7037(69)90126-4.

Olson, P., G. Schubert, and C. Anderson (1993), Structure of axisymmetric mantle plumes, *J. Geophys. Res.*, *98*, 6829–6844, doi:10.1029/92JB01013.

Pertermann, M., M. M. Hirschmann, K. Hametner, D. Gunther, and M. W. Schmidt (2004), Experimental determination of trace element partitioning between garnet and silica-rich liquid during anhydrous partial melting of MORB-like eclogite, *Geochem. Geophys. Geosyst.*, *5*, Q05A01, doi:10.1029/2003GC000638.

Pietruszka, A. J., and M. O. Garcia (1999), A rapid fluctuation in the mantle source and melting history of Kilauea Volcano inferred from the geochemistry of its historical summit lavas (1790–1982), *J. Petrol.*, *40*(8), 1321–1342, doi:10.1093/petrology/40.8.1321.

Plank, T., and C. H. Langmuir (1998), The chemical composition of subducting sediment and its consequences for the crust and mantle, *Chem. Geol.*, *145*(3–4), 325–394, doi:10.1016/S0009-2541(97)00150-2.

Quane, S. L., M. O. Garcia, H. Guillou, and T. P. Hulsebosch (2000), Magmatic history of the East Rift Zone of Kilauea Volcano, Hawaii based on drill core from SOH 1, *J. Volcanol. Geotherm. Res.*, *102*(3–4), 319–338, doi:10.1016/S0377-0273(00)00194-3.

Ray, J. S., M. W. Martin, J. Veizer, and S. A. Bowring (2002), U-Pb zircon dating and Sr isotope systematics of the Vindhyan Supergroup, India, *Geology*, *30*(2), 131–134, doi:10.1130/0091-7613(2002)030<0131:UPZDAS>2.0.CO;2.

Regelous, M., Y. Niu, J. I. Wendt, R. Batiza, A. Greig, and K. D. Collerson (1999), Variations in the geochemistry of magmatism on the East Pacific Rise at 10 degrees 30′N since 800 ka, *Earth Planet. Sci. Lett.*, *168*(1–2), 45–63, doi:10.1016/S0012-821X(99)00048-5.

Regelous, M., A. W. Hofmann, W. Abouchami, and S. J. G. Galer (2003), Geochemistry of lavas from the Emperor Seamounts, and the geochemical evolution of Hawaiian magmatism from 85 to 42 Ma, *J. Petrol.*, *44*, 113–140, doi:10.1093/petrology/44.1.113.

Ren, Z.-Y., S. Ingle, E. Takahashi, N. Hirano, and T. Hirata (2005), The chemical structure of the Hawaiian mantle plume, *Nature*, *436*, 837–840, doi:10.1038/nature03907.

Rhodes, J. M. (1995), The 1852 and 1868 Mauna Loa picrite eruptions: Clues to parental magma compositions and the magmatic plumbing system, in *Mauna Loa Revealed: Structure, Composition, History, and Hazards*, *Geophys. Monogr. Ser.*, vol. 92, edited by J. M. Rhodes and J. P. Lockwood, pp. 241–262, AGU, Washington, D. C.

Rhodes, J. M. (1996), Geochemical stratigraphy of lava flows sampled by the Hawaii Scientific Drilling Project, *J. Geophys. Res.*, *101*, 11,729–11,746, doi:10.1029/95JB03704.

Rhodes, J. M., and S. R. Hart (1995), Episodic trace element and isotopic variation in historical Mauna Loa lavas, in *Mauna Loa Revealed: Structure, Composition, History, and Hazards*, *Geophys. Monogr. Ser.*, vol. 92, edited by J. M. Rhodes and J. P. Lockwood, pp. 263–288, AGU, Washington, D. C.

Rhodes, J. M., and M. J. Vollinger (2004), Composition of basaltic lavas sampled by phase-2 of the Hawaii Scientific Drilling Project: Geochemical stratigraphy and magma types, *Geochem. Geophys. Geosyst.*, *5*, Q03G13, doi:10.1029/2002GC000434.

Ribe, N. M., and U. R. Christensen (1999), The dynamical origin of Hawaiian volcanism, *Earth Planet. Sci. Lett.*, *171*, 517–531, doi:10.1016/S0012-821X(99)00179-X.

Ridgwell, A., and R. E. Zeebe (2005), The role of the global carbonate cycle in the regulation and evolution of the Earth system, *Earth Planet. Sci. Lett.*, *234*, 299–315, doi:10.1016/j.epsl.2005.03.006.

Robinson, J. E., and B. W. Eakins (2006), Calculated volumes of individual shield volcanoes at the young end of the Hawaiian Ridge, *J. Volcanol. Geotherm. Res.*, *151*, 309–317, doi:10.1016/j.jvolgeores.2005.07.033.

Roden, M. F., F. A. Frey, and D. A. Clague (1984), Geochemistry of tholeiitic and alkalic lavas from the Koolau Range, Oahu, Hawaii: Implications for Hawaiian volcanism, *Earth Planet. Sci. Lett.*, *69*(1), 141–158, doi:10.1016/0012-821X(84)90079-7.

Roden, M. F., T. Trull, S. R. Hart, and F. A. Frey (1994), New He, Sr, Nd and Pb isotopic constraints on the constitution of the Hawaiian plume: Results from Koolau Volcano, Oahu, Hawaii, *Geochim. Cosmochim. Acta*, *58*, 1431–1440, doi:10.1016/0016-7037(94)90547-9.

Salters, V. J. M. (1996), The generation of mid-ocean ridge basalts from the Hf and Nd isotope perspective, *Earth Planet. Sci. Lett.*, *141*, 109–123, doi:10.1016/0012-821X(96)00070-2.

Salters, V. J. M., and J. Longhi (1999), Trace element partitioning during the initial stages of melting beneath mid-ocean ridges, *Earth Planet. Sci. Lett.*, *166*, 15–30, doi:10.1016/S0012-821X(98)00271-4.

Salters, V. J. M., and A. Stracke (2004), Composition of the depleted mantle, *Geochem. Geophys. Geosyst.*, *5*, Q05B07, doi:10.1029/2003GC000597.

Salters, V. J. M., J. Longhi, and M. Bizimis (2002), Near mantle solidus trace element partitioning at pressures up to 3.4 GPa, *Geochem. Geophys. Geosyst.*, *3*(7), 1038, doi:10.1029/2001GC000148.

Salters, V. J. M., J. Blichert, Z. Fekiacova, A. Sachi-Kocher, and M. Bizimis (2006), Isotope and trace element evidence for depleted lithosphere in the source of enriched Koolau basalts, *Contrib. Mineral. Petrol.*, *151*, 297–312, doi:10.1007/s00410-005-0059-y.

Samuel, H., and C. G. Farnetani (2003), Thermochemical convection and helium concentrations in mantle plumes, *Earth Planet. Sci. Lett.*, *207*, 39–56, doi:10.1016/S0012-821X(02)01125-1.

Shields, G., and J. Veizer (2002), Precambrian marine carbonate isotope database: Version 1.1, *Geochem. Geophys. Geosyst.*, *3*(6), 1031, doi:10.1029/2001GC000266.

Sobolev, A. V., A. W. Hofmann, and I. K. Nikogosian (2000), Recycled oceanic crust observed in ghost plagioclase within the source of Mauna Loa lavas, *Nature*, *404*, 986–990, doi:10.1038/35010098.

Sobolev, A. V., A. W. Hofmann, S. V. Sobolev, and I. K. Nikogosian (2005), An olivine-free mantle source of Hawaiian shield basalts, *Nature*, *434*, 590–597, doi:10.1038/nature03411.

Sobolev, A. V., et al. (2007), The amount of recycled crust in sources of mantle-derived melts, *Science*, *316*, 412–417, doi:10.1126/science.1138113.

Stille, P., D. M. Unruh, and M. Tatsumoto (1983), Pb, Sr, Nd and Hf isotopic evidence of multiple sources for Oahu, Hawaii basalts, *Nature*, *304*(5921), 25–29, doi:10.1038/304025a0.

Stolper, E., S. Sherman, M. Garcia, M. Baker, and C. Seaman (2004), Glass in the submarine section of the HSDP2 drill core, Hilo, Hawaii, *Geochem. Geophys. Geosyst.*, *5*, Q07G15, doi:10.1029/2003GC000553.

Tanaka, R., A. Makishima, and E. Nakamura (2008), Hawaiian double volcanic chain triggered by an episodic involvement of recycled material: Constraints from temporal Sr-Nd-Hf-Pb isotopic trend of the Loa-type volcanoes, *Earth Planet. Sci. Lett.*, *265*, 450–465, doi:10.1016/j.epsl.2007.10.035.

Tatsumoto, M., E. Hegner, and D. M. Unruh (1987), Origin of the West Maui volcanic rocks inferred from Pb, Sr, and Nd isotopes and a multicomponent model for oceanic basalt, in *Volcanism in Hawaii*, vol. 2, edited by R. W. Decker, T. L. Wright, and P. H. Stauffer, *U.S. Geol. Surv. Prof. Pap.*, *1350*, 723–744.

Veizer, J., J. Hoefs, D. R. Lowe, and P. C. Thurston (1989), Geochemistry of Precambrian carbonatites: II. Archean greenstone belts and Archean sea water, *Geochim. Cosmochim. Acta*, *53*, 859–871, doi:10.1016/0016-7037(89)90031-8.

Vervoort, J. D., P. J. Patchett, J. Blichert-Toft, and F. Albarede (1999), Relationships between Lu-Hf and Sm-Nd isotopic systems in the global sedimentary system, *Earth Planet. Sci. Lett.*, *168*, 79–99, doi:10.1016/S0012-821X(99)00047-3.

Walter, M. J. (1998), Melting of garnet peridotite and the origin of komatiite and depleted lithosphere, *J. Petrol.*, *39*(1), 29–60, doi:10.1093/petrology/39.1.29.

West, H. B., D. C. Gerlach, W. P. Leeman, and M. O. Garcia (1987), Isotopic constraints on the origin of Hawaiian lavas from the Maui volcanic complex, Hawaii, *Nature*, *330*(6145), 216–220, doi:10.1038/330216a0.

White, W. M., F. Albarède, and P. Télouk (2000), High-precision analysis of Pb isotopic ratios using multi-collector ICP-MS, *Chem. Geol.*, *167*, 257–270, doi:10.1016/S0009-2541(99)00182-5.

Workman, R. K., and S. R. Hart (2005), Major and trace element composition of the depleted MORB mantle (DMM), *Earth Planet. Sci. Lett.*, *231*, 53–72, doi:10.1016/j.epsl.2004.12.005.

Xu, G., F. A. Frey, D. A. Clague, D. Weis, and M. H. Beeson (2005), East Molokai and other Kea-trend volcanoes: Magmatic processes and sources as they migrate away from the Hawaiian hot spot, *Geochem. Geophys. Geosyst.*, *6*, Q05008, doi:10.1029/2004GC000830.

Xu, G., F. A. Frey, D. A. Clague, W. Abouchami, J. Blichert-Toft, B. Cousens, and M. Weisler (2007a), Geochemical characteristics of West Molokai shield- and postshield-stage lavas: Constraints on Hawaiian plume models, *Geochem. Geophys. Geosyst.*, *8*, Q08G21, doi:10.1029/2006GC001554.

Xu, G., J. Blichert-Toft, D. A. Clague, B. Cousens, F. A. Frey, and J. G. Moore (2007b), Penguin Bank: A Loa-trend Hawaiian volcano, *Eos. Trans. AGU*, *88*(52), Fall Meet. Suppl., Abstract V33A-1174.

Yang, H.-J., F. A. Frey, J. M. Rhodes, and M. O. Garcia (1996), Evolution of Mauna Kea volcano: Inferences from lava compositions recovered in the Hawaii Scientific Drilling Project, *J. Geophys. Res.*, *101*, 11,747–11,767, doi:10.1029/95JB03465.

Zimmer, M., A. Kroener, K. P. Jochum, T. Reischmann, and W. Todt (1995), The Gabal Gerf Complex: A Precambrian N-MORB ophiolite in the Nubian Shield, NE Africa, *Chem. Geol.*, *123*(1–4), 29–51, doi:10.1016/0009-2541(95)00018-H.